INTERNATIONAL ATOMIC ENERGY AGENCY
UNITED NATIONS EDUCATIONAL, SCIENTIFIC AND CULTURAL ORGANIZATION

INTERNATIONAL CENTRE FOR THEORETICAL PHYSICS
34100 TRIESTE (ITALY) - P.O.B. 586 - MIRAMARE - STRADA COSTIERA 11 - TELEPHONE 2240-1
CABLE CENTRATOM - TELEX 460392-I

SMR/169 - 6

WORKSHOP ON OPTICAL FIBER COMMUNICATION
(24 February - 21 March 1986)

OPTICAL FIBER MEASUREMENTS.

F.M. SMOLKA
Optical Fiber Division
CPqD/TELEBRAS
Campinas, SP, 13100
Brazil

OPTICAL FIBER MEASUREMENTS

FRANCISCO MARTIM SMOLKA

Optical Fiber Division

CPqD/TELEBRAS

Campinas, SP, 13100, BRAZIL

February 1986

Lecture Notes prepared for the
Workshop on Optical Fiber Communication
held at the International Centre for Theoretical Physics
Trieste, Italy

TELECOMUNICAÇÕES BRASILEIRAS S.A. TELEBRÁS
(VINCULADA AO MINISTÉRIO DAS COMUNICAÇÕES)

CONTENTS

1. INTRODUCTION

The history of modern fiber optics technology started about 15 years ago when low loss silica based glass fiber was first realized. Industrial production as well as first trials systems started around 10 years ago. Commercial operation of optical communication networks got under way in the last five years but the fully implementation of this technology will happen over the next decade.

Since the begining, optical fiber measurement was a critical issue due to various aspects such as:

1. fiber's very small transversal dimensions, in the microns range;
2. necessity of measuring very small losses, down to 0.1 dB/Km with 1% accuracy;
3. fiber bandwidth increasing very rapidly, from the tens of MHz.Km to the GHz.Km region;
4. some of the fiber characteristics depending very critically on fiber structure and materials;
5. difficulty of extending individual parameters to long length concatenated fibers, for systems applications;
6. need to produce a large amount of different type of data very fast and with good accuracy to help basic fabrication research and also in the commercial manufacturing environment.

To attend all those needs and others, a large number of techniques were developed. Among these, only a limited set are pratically applied. In these lectures, we will give special attention to those methods that were proven necessary for

optical fiber production, cabling and installation.

Measurements of optical fibers can be divided in two main types:

a) fiber structural characteristics such as geometry, length, index of refraction profile and chemical composition;
b) transmission properties as attenuation, bandwidth, chromatic dispersion, numerical aperture and monomodal operation characteristics.

Generally, these two sets of results are correlated since the transmission properties depend on the structural characteristics. These last ones, are measured locally as for example, in both ends of a reel of various kilometers of continuous fiber. On the other end,the transmission properties are in some sense averaged over the whole length of the fiber. So in this context, the question of a steady state situation arises. How is the transmission data depending on the length of a uniform measured fiber? Considering also, that in practice the fibers are not totally uniform along its length, well defined correlations, between structural and transmission data are not always easy to achieve. This is why, that in most situations, every fiber that comes out of a production line has to be measured.

Optical fiber measurement techniques must attend two types of customers.One of them is the people involved in fiber research and manufacturing and the other is the final user. The first one needs informations that will help preform fabrication and fiber drawing while the other is only concerned about the total loss and bandwidth of the optical link. Tables 1 and 2 are a summary

of the type of information that is needed for each case which optical measurements will yield it. Only the more standard measurement techniques are listed.

TABLE 1

OPTICAL MEASUREMENTS FOR FIBER RESEARCH/MANUFACTURING

PROCESS	INFORMATION	TYPE OF FIBER MEASUREMENT
Preform Fabrication	Core/cladding geometry	Preform and fiber geometry
	Dopants control	Preform and fiber index of refraction profile Fiber bandwidth Chromatic dispersion
	Impurities	Spectral loss curve
	Bubbles and defects. Uniformity along preform/fiber length	Local attenuation along fiber length (Optical Time Domain Reflectometry - OTDR)
Fiber Drawing	Coating and fiber geometry	Fiber geometry
	Fiber diameter control Coating properties Drawing tension Winding tension	Spectral loss curves

TABLE 2

OPTICAL MEASUREMENT FOR FIBER USER

	INFORMATION	TYPE OF FIBER MEASUREMENT
Total Loss	Individual fiber loss	Spectral loss curve
	Splice and cabling losses	Fiber geometry Index of refraction profile Attenuation Monomodal mode field diameter
	Light source coupling to fiber	Fiber geometry Index of refraction profile Numerical aperture
Total Bandwidth	Individual fiber bandwidth	Fiber bandwidth
	Concatenation effects	Fiber bandwidth of spliced fibers Index of refraction profile Fiber geometry
	Chromatic effects	Chromatic dispersion
	Monomodal operation	Cut off wavelength

In the text that follows, each of the fiber measurements techniques mentioned in Tables 1 and 2 will be described in details. Much of the information contained here is based in the experience acquired during the research work for developing optical fiber technology at the Telebras Research Center (Brazil). The basic bibliography and references for the contents given here, are listed in the end of the text and so no particular citation will be given. The experimental results, shown in the figures were obtained in Telebras R&D labs.

2. PREFORM AND FIBER GEOMETRY MEASUREMENT

In Figure 1 the cross section of a typical optical fiber is shown. From it, the following fiber geometry parameters can be defined:

core diameter - $\phi_n = (a+b)/2$

clad diameter - $\phi_c = (A+B)/2$

core non-circularity - $\epsilon_n = \dfrac{(a-b)}{\phi_n}$

clad non-circularity - $\epsilon_c = \dfrac{(A-B)}{\phi_c}$

core-clad concentricity error - $C_c = t/\phi_n$

coating diameter - D

fiber-coating concentricity - $C_f = L</L>$

The most direct way of obtaining the above parameters, is to observe a short piece of fiber, through a inverted microscope preferably. The ends of the fiber must be carefully cleaved using a scribe and bending method. The microscope must be provided with a calibrated reticle. A precision of about 1 to 2 microns is usually obtained with carefull procedures.

Depending on the index of refraction of the coating material, there will be more or less light guided in the cladding of the

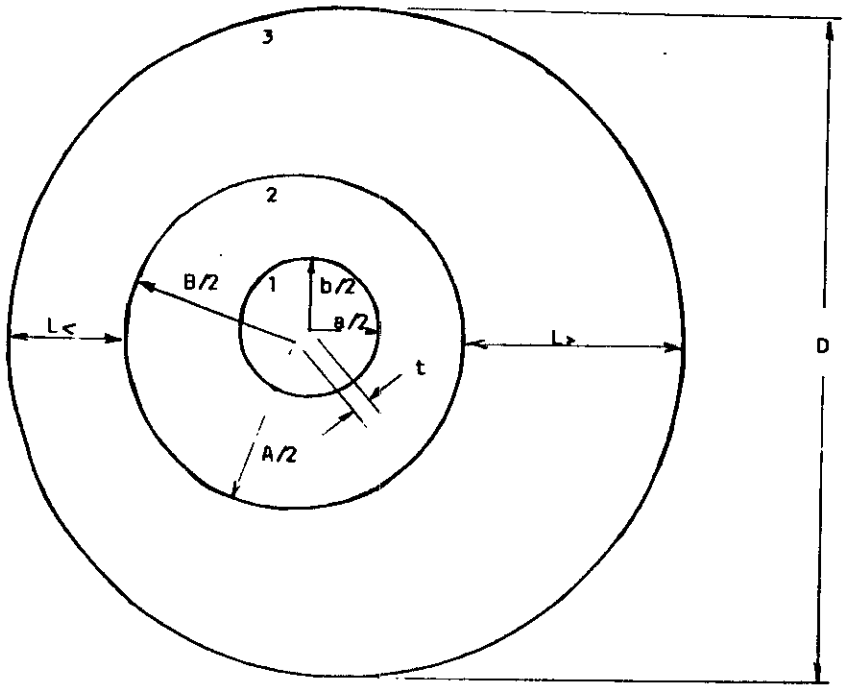

1 - core
2 - cladding
3 - coating

FIG. 1 - Optical fiber geometrical parameters.

fiber. This is because the cladding and the coating can form a secondary waveguide if the index of refraction of the coating is lower than that of pure silica (n=1.46). Thus, for coatings that have a high index of refraction, the luminosity of the fiber cladding, in the microscope, can be controled by using a shorter length of fiber.

When we need a more precise measurement, and for fibers that have a graded index profile, where the core-cladding interface is not very sharp, the core's diameter is measured from the index of refraction profile. There are several ways of obtaining this profile as will be seen later. In this section, we will be concentrated on techniques that are more aplicable for extracting the geometrical parameters, described above, that need a two dimensional view of the fiber end.

As shown in the next section, when a short length of fiber is illuminated by a Lambertian source, the light intensity distribution at the near field region or accross an image of the fiber face, is proportional to the index of refraction profile. Thus, by using the experimental set-up shown in Figure 2, a two dimensional intensity display of the fiber face can be obtained. A length of about 1-2m of fiber is illuminated by a light source with the use of a microscope objective. On the other end, a image of the fiber face is formed on a TV camera by another microscope objective. The intensity along a given scan line can be acquired with a video digitizer and stored in a computer as shown in Figure 2. The two core-clad interface points are defined at a given intensity height, for example, 5%. In a similar way, the

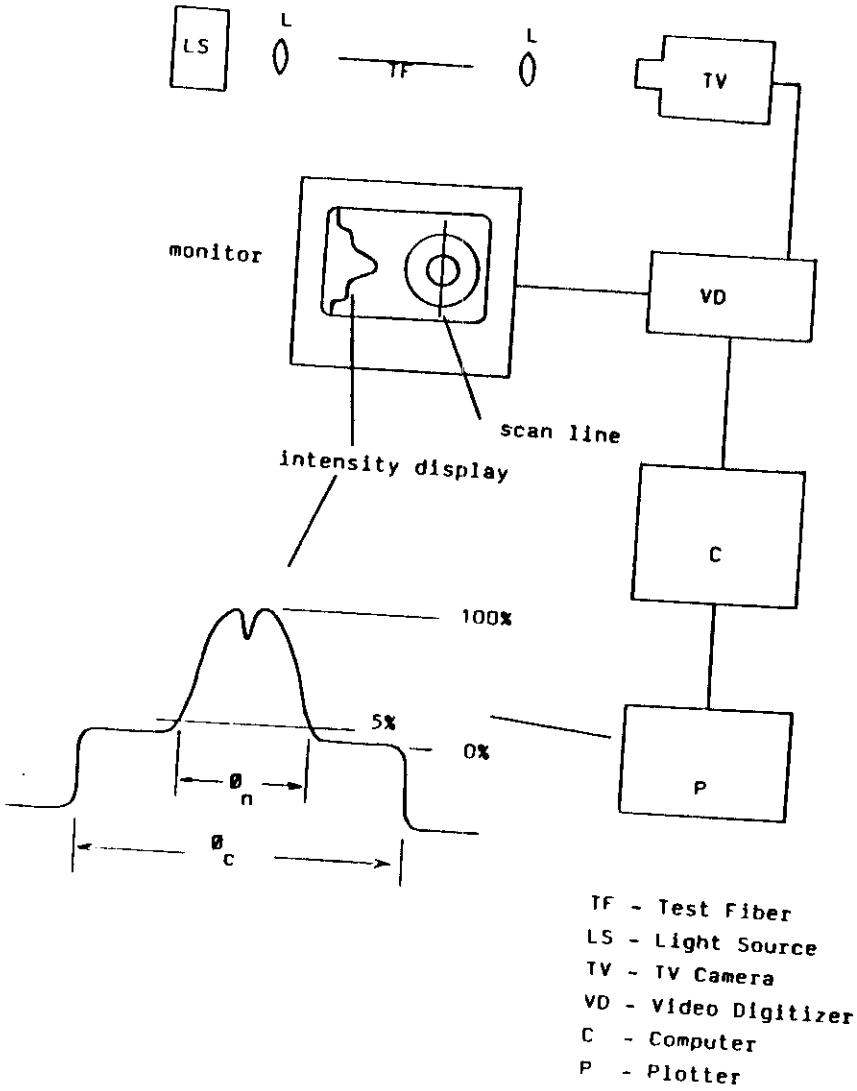

FIG. 2 - Measurement system for determination of fiber geometry

outside points are also defined. By scanning all the fiber image, the contour of the core and cladding is obtained. It is then possible to define two ellipses: one that best fits (least square criterium) the contour points of the cladding and another one that best fits the equivalent points of the core.The precision of this technique is around 0.5 microns.

The methods described above can be applied to multimode and monomode fibers. For these last ones, care must be taken to use a light source with a wavelength much shorter than the cut-off wavelength of the fiber. Since most monomode fibers are designed for λ_c > 1.2 microns or above, illuminating the fiber with a 0.5 microns light, secures that the measurement is made in the multimode regime so the nearest to the true value of the core diameter is measured.

Determining the geometrical parameters of a preform requires a little more work on sample preparation. The most obvious way is to slice a 1-2mm piece of the preform, give it a fast polishing to get a better surface and then measured it with a normal microscope equipped with a reticle. But this technique, apart from being destructive,gives only information at one position along the preform. To circunvent this problem, and get information along the whole length of the preform, one may immersed it, in a liquid with the same index of refraction of the cladding and inspect under a low magnification microscope as shown in Figure 3. In this manner, only the core-cladding interface and inner core structure are visible. By rotating and translating the whole preform, measurements can be performed over

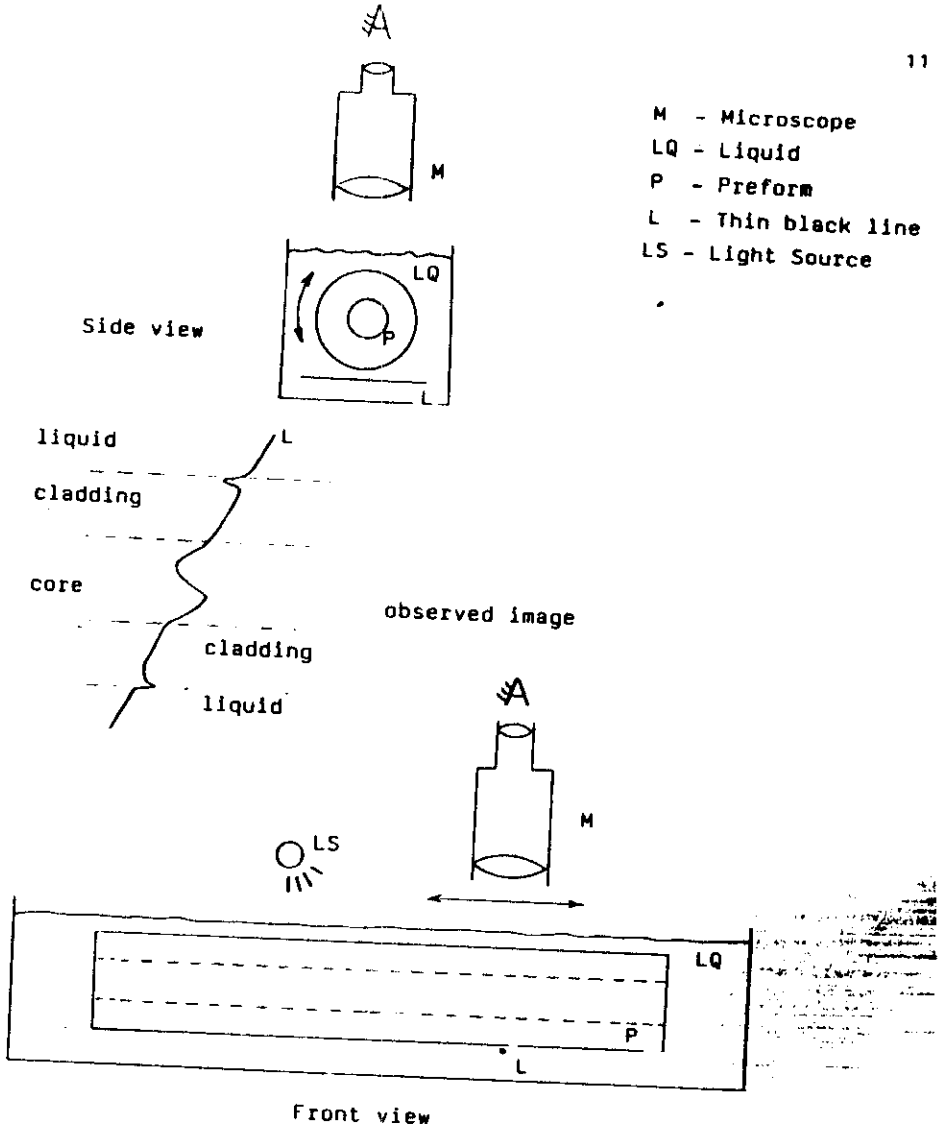

M - Microscope
LQ - Liquid
P - Preform
L - Thin black line
LS - Light Source

FIG. 3 - Non-destructive method for observing the geometrical characteristics of a preform.

all its length. Placing a thin dark line under the preform can improved the visibility of the core's structure. This method is valuable in determine the part of the preform, where the core diameter is uniform, since most MCVD made preform exibits ends effects where the core diameter is smaller.

Finally, a more exact and also expensive way of getting geometrical informations, is to measure the index-profile in the preform by using commercial equipments that employ light deflection techniques described in the next section. This way one gets in general,a one dimensional plot of the index of refraction at one point along the preform, like the one shown in Figure 4, from which geometrical information can be extracted. More sophisticated two dimensional profiling is also possible but requires a lot of data processing.

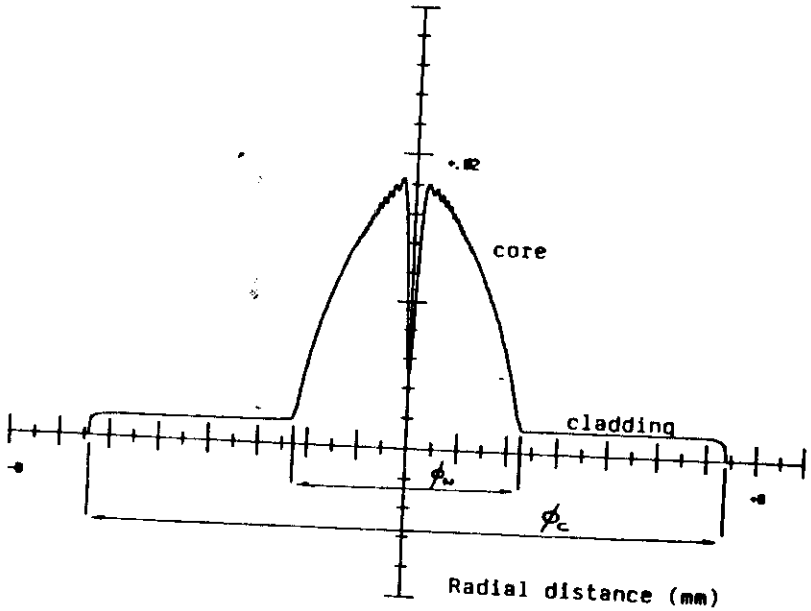

FIG. 4 - Geometrical measurements in a preform using the index of refraction profile.

3. MEASUREMENTS OF THE INDEX OF REFRACTION PROFILE

3.1. INTRODUCTION

The bandwidth of a multimode graded index fiber is determined by the index of refraction profile of the fiber core. A near parabolic index of refraction profile with amplitude Δn_o maximize the bandwidth. Small deviations (1% of the Δn_o) from this ideal profile can deteriorate the bandwidth. To be effective as diagnostic tool to improve the bandwidth the method of index profiling has to have a accuracy better than $\delta n \sim 1\% \Delta n_o \sim 10^{-4}$ x 1.455.

Several techniques were developed but only a few of them turned to be practical and accepted for routine measurements. The most widely used, is the transmitted near field scanning because of its simplicity. But this method gives only a qualitative view of the profile and it suffers from problems of transmissions of non guided modes that may distort the measured profile. But apart from these, is well suited for a fast glance at the profile and to obtain geometrical information.

To solve this transmission problem, researchers moved to techniques that measures the profile locally. Interferometric techniques in which a small sample of fiber is examined is an example of this. Another is the refracted near field that relies on the light acceptance properties at one end of length of fiber. So, these are the three basic techniques that we will discuss in this chapter.

3.2. NEAR FIELD SCANNING

This technique relies on the fact that the power distribution on the exit face of fiber is proportional to the index of refraction distribution when the input end is excited by a Lambertian source. Let's prove this.

A Lambertian source emits radiation according to

$$I(\theta) = I_o \cos(\theta) \qquad (1)$$

where θ is the angle between the perpendicular to the plane of the source and the emission direction. Most incoherent sources like a LED or heated metal emits according to this law.

For any point in the fiber core, the light is guided if it's confined in a cone (θ_m) defined by the local numerical aperture

$$NA(r) = \sqrt{n(r)^2 - n_o^2} = \sin\theta_m(r) \qquad (2)$$

where n_o is the cladding index of refraction and n(r) the index profile of the core. Thus the light intensity accepted into the cone defined by θ_m is

$$P(r) = \int I(\theta)\, d\Omega \qquad (3)$$

or

$$P(r) = \int_0^{2\pi} d\phi \int_0^{\theta_m} I_o \cos\theta \sin\theta \, d\theta \qquad (4)$$

so

$$\frac{P(r)}{P(o)} = \frac{\sin^2\theta_m(r)}{\sin^2\theta_m(o)} \qquad (5)$$

where we normalized P(r) to intensity at the center of the fiber.

Using (2) and the fact that $n(r) \sim n_o$ then (5) can be transformed to

$$\frac{P(r)}{P(o)} = \frac{\Delta n(r)}{\Delta n_o} \qquad (6)$$

where $\Delta n(r)$ is the index difference between core and cladding.

If we consider that all the excited modes have the same attenuation over a given length of the fiber, the light intensity at the output face will be also given by (6), thus, scanning the near field one gets the index profile $\Delta n(r)$. But since the near field is defined at a distance of the order of the wavelength of radiation we don't have a direct access to this distribution. What is normally done is to produce a good quality magnified image of the end face and scan it with a small detector as shown in Figure 5. Normally we use a chopped light with a lock-in amplifier to improve signal to noise ratio. An important detail concerns the optics that controls the launching of light into the fiber. To be sure that all modes are excited the spot size focused at the input face must be larger than the fiber core and

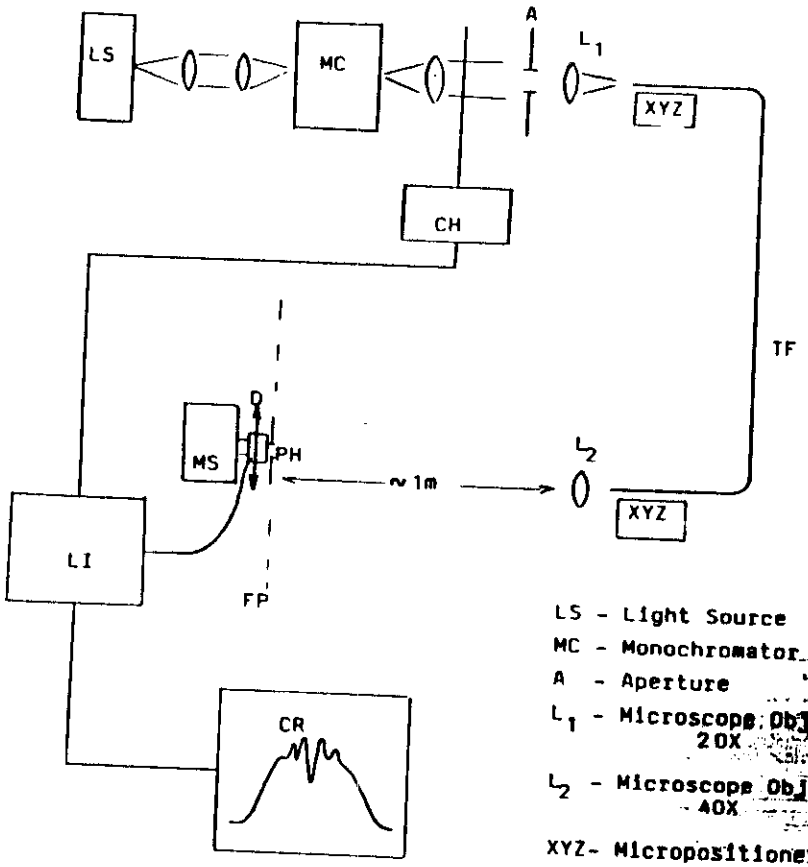

LS - Light Source
MC - Monochromator
A - Aperture
L_1 - Microscope Objective 20X
L_2 - Microscope Objective 40X
XYZ- Micropositioner
CH - Chopper
LI - Lock-in Amplifier
MS - Motorized Scanner
D - Detector
PH - Pin Hole 50 microns
FP - Focusing Plane
TF - Test Fiber 1~2 m
CR - Chart Recorder

FIG. 5 - Measuring system for obtaining the index of refraction profile by the near field method.

have a numerical aperture exceeding that of the test fiber. Note that this arrangement is very similar to that one described in Figure 2 where only geometrical data was of interest.

A typical result obtained with the set-up of Figure 5, is shown in Figure 6. If one wishes, several scans can be done at different lines accross the image. Normally the scan passes through the center so useful information about the dip of MCVD fibers, is acquired. The dip or other structural detail can be used to properly focus the image on the scan plane.

Once the profile is obtained, a least square fit to a given mathematical expression can be done. In section 3.6 we will illustrate this point. Two of the assumptions made in the derivation of Eq. (6), where that only bound modes are excited and they all have the same attenuation. In practice, other modes called leaky rays can be excited and not be completely attenuated over the fiber length. This is a particularly important issue for step index fibers, where information in the region between 50 and 90% of the fiber radius is distorted. If we use a longer fiber, to cut off leaky rays, differential attenuation between the guided modes, will also have deleterious effects. For fibers with a near parabolic profile, leaky rays doesn't seems do be a problem.

From (6), we note that a quantitative value of the index of refraction is not obtained with this technique. If in the other hand, the far field is scanned, this information is available. Since every point in the fiber end face will radiate into a cone given by the local numerical aperture, from (2) we see that the

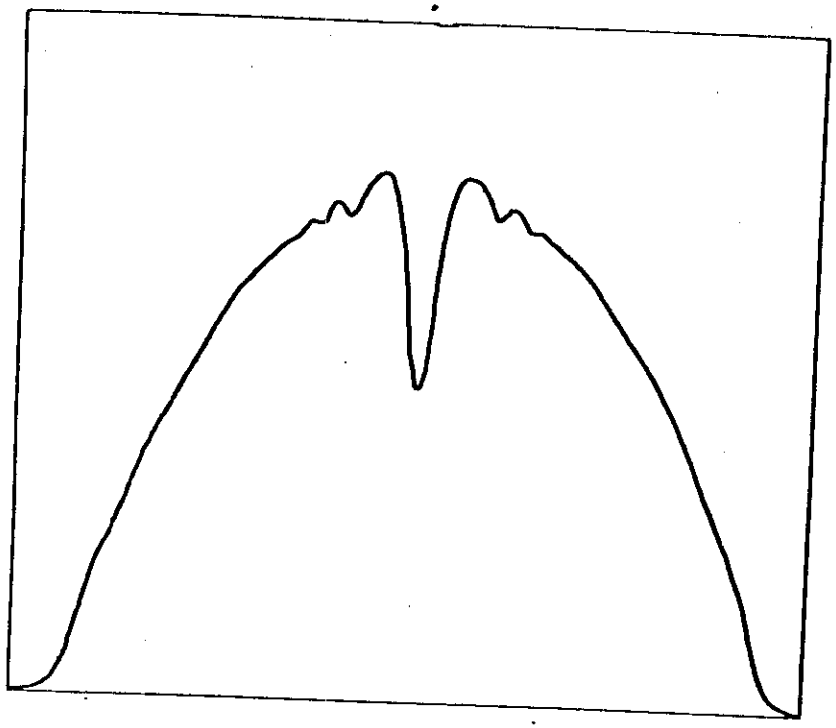

FIG. 6 - Near field scan for a graded index multimode fiber.

maximum radiation angle is

$$NA = \sin\Theta_{max} = \sqrt{n^2(r=o) - n_o^2} = 2 n_o \Delta n(o) \quad (7)$$

so by measuring Θ_{max} and knowing n_o, $n(o)$ is determined. The apparatus for performing this measurement is described in Figure 7. The launch optics is the same as in Figure 5, and the angular detection resolution is about 0.5^o as seen for the fiber face..Once n_o is known, the vertical scale in the near field can be calibrated. Please note that this is a rough calibration, and for a more accurate result, the other index of refraction measurement methods must be used.

All that has been said above, about near field scanning, applies to multimode fibers where hundreds of modes are excited. When only a few modes are allowed, the spatial resolution is lost, because of the spatial extent of the modes themselves. Thus, using near field technique with monomode fibers will not provided the real index of refraction profile. This technique is used with these type of fiber, in the context of determining the spot size of the fundamental mode as we be seen in section 6.4.

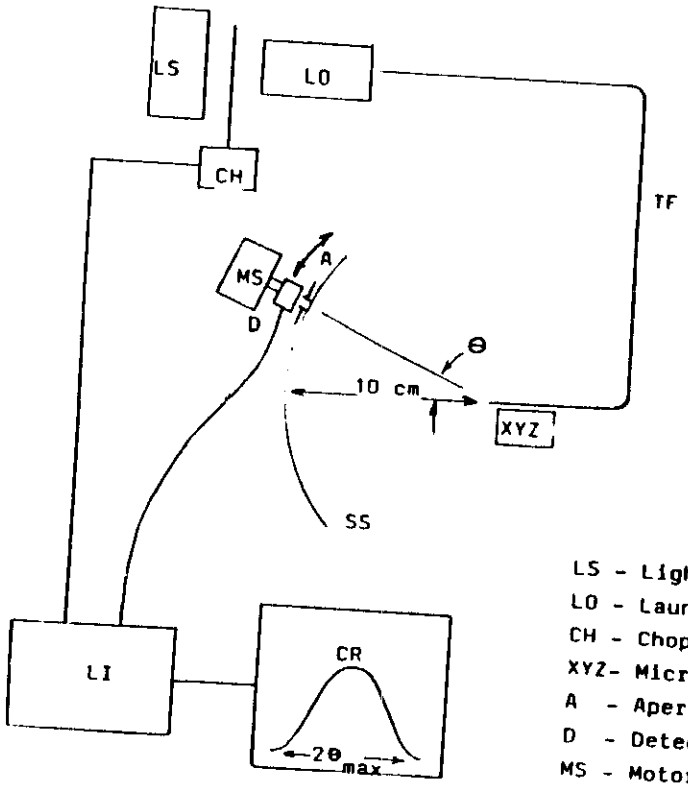

FIG. 7 - Experimental set-up for far field scanning.

3.3. REFRACTED NEAR FIELD SCANNING

In the last section, we have seen that the amount of light trapped in the fiber as a function of position was proportional to the index of refraction. Conversely, if we illuminated the fiber with a beam that has an output cone greater than the acceptance angle of the fiber and measure the amount of light that is not guided, we are also able to get information about the index profile. The description of the method given bellow, is based on Marcuse's boook on optical fiber measurement listed on the bibliography to this text.

Consider Figure 8a and let us follow a non guided ray through the fiber imersed in a liquid with index of refraction n_e. From Snell's law, at points 1 and 2 we have

$$n_e \sin\Theta_1 = n_f \sin\Theta_f \qquad (8)$$

and

$$n_f \sin\left(\frac{\pi}{2} - \Theta_f\right) = n_e \sin\left(\frac{\pi}{2} - \Theta_2\right) \qquad (9)$$

or

$$n_f \cos\Theta_f = n_e \cos\Theta_2 \qquad (10)$$

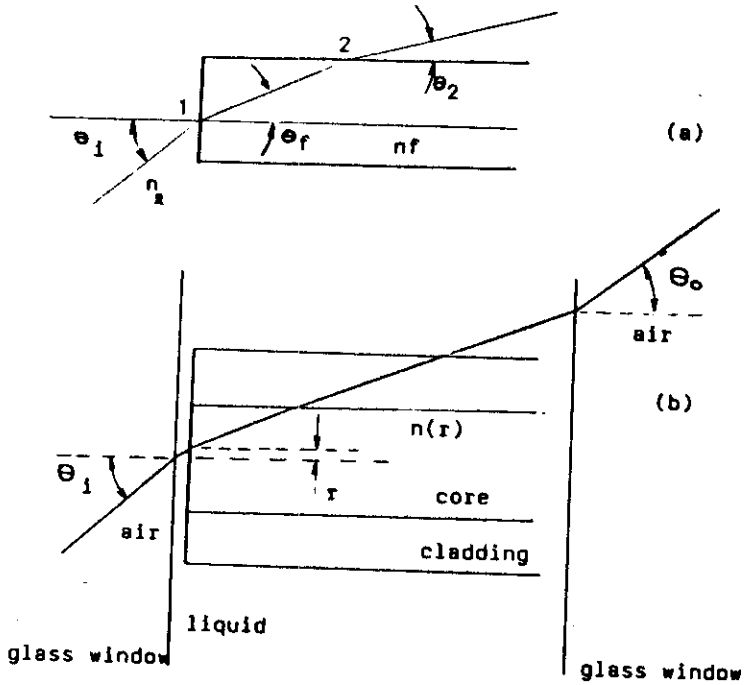

FIG. 8 - Basic geometry for the refracted near field technique.

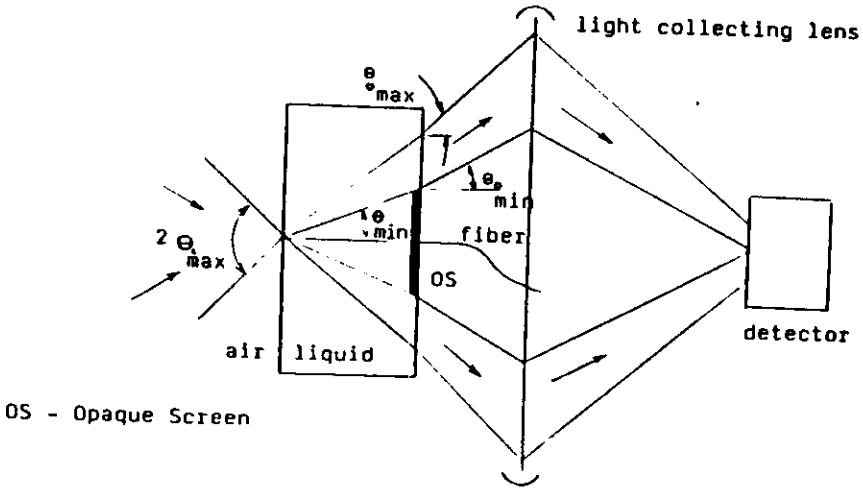

OS - Opaque Screen

FIG.9 - Refracted near field measuring cell.

Eliminating Θ_f from (10) and (8) we have

$$n_e \sin\Theta_i = \left[n_f^2 - n_e^2 + n_e^2 \sin^2\Theta_2 \right]^{1/2} . \quad (11)$$

that is, a relation between the input and output angles and the fiber index of refraction.

For a more general case, when the fiber has a non-constant index of refraction distribution and is placed between two glass plates filled with liquid, a relation similar to (11) can be derived, namely

$$n^2(r) = n_e^2 + \sin^2\Theta_i - \sin^2\Theta_o \quad (12)$$

Instead of measuring the two angles Θ_i and Θ_o, let us focus at the fiber face, a beam with a given cone angle and measure the total optical power between two output angles $\Theta_{o\,max}$ and $\Theta_{o\,min}$ as shown in Figure 9. The opaque screen is used to eliminate the quasi bound modes, the so called leaky rays, that where a source of problems for the transmitted near field technique. Assuming that the light distribution in the focused spot, in the entrance face of the fibe, is Lambertian (see Eq. 1), the total power between $\Theta_{o\,max}$ and $\Theta_{o\,min}$ is

$$P(r) = \int_{\Omega_{min}}^{\Omega_{max}} I_o \cos\theta \, d\Omega \qquad (13)$$

or

$$P(r) = I_o \int_0^{2\pi} d\phi \int_{\theta_{i\,min}}^{\theta_{i\,max}} \cos\theta \sin\theta \, d\theta \qquad (14)$$

where $\theta_{i\,min}$ and $\theta_{i\,max}$ are related to $\theta_{o\,min}$ and $\theta_{o\,max}$ by Equation (12). The result is then

$$P(r) = I_o \cdot \pi \left[\sin^2\theta_{i\,max} - \sin^2\theta_{o\,min} - \frac{\left(n^2(r) - n_e^2\right)}{n_g^2} \right] \qquad (15)$$

When the focused light beam is incident not on the fiber but at the liquid, P is a constant given by

$$P_e = I_o \cdot \pi \cdot (\sin^2\theta_{i\,max} - \sin^2\theta_{o\,min}) \qquad (16)$$

thus Eq. 15 can be written as

$$n^2(r) - n_e^2 = n_e^2 (\sin^2\theta_{i\,max} - \sin^2\theta_{o\,min}) \frac{\left(P_e - P(r)\right)}{P_e} \qquad (17)$$

For a given experimental configuration, $\theta_{i\,max}$, $\theta_{o\,min}$ and n_e are fixed, so from (17)

$$\Delta n(r) = C \frac{\left[P_e - P(r)\right]}{P_e} \qquad (18)$$

where $\Delta n(r) = n(r) - n_e$. The constant C can be obtained by making a measurement using a step index fiber (n(r) = constant) with a known index of refraction.

The size of the screen or the value of $\theta_{o\,min}$ must be such that it blocks the collection of light from the leaky rays. It can be shown that

$$\theta_{o\,min} > \tan^{-1}\sqrt{2\Delta} \qquad (19)$$

where

$$\Delta = \left(n_{max}(r) - n_o\right)/n_o$$

is the maximum relative index of refraction of the fiber.

For multimode fibers, $\Delta < 1.5\%$ so $\theta_{o\,min} > 10^{o}$. Going back to (12) we see that $\sin \theta_{i\,max} > 0.3$ in order that $\theta_{o\,max} > \theta_{o\,min}$ and have a non zero detected power. In other words, we need to use a very high numerical aperture focused beam, at the fiber input face.

A practical implementation of the method is shown in Figure 10. The light source is a spatially filtered laser beam in order to have the smaller possible spot size at the fiber face. In reality this is a Gaussian and not a Lambertian beam but in practice very small errors are induced because in first approximation they are the same. The fiber is placed inside a cell with liquid that have an index of refraction close to that of silica. The cell windows are a very thin microscope slide so the fiber is positioned at the focal plane of the microscope objective. The opaque disk is placed behind the cell close to the condensing lens assembly that collects the refracted light and focused it on the face of a detector. The whole cell can be moved with respect to the light beam, with the help of high precision micropositioners (resolution better than 1 micron), so the spot is scanned across the fiber. The other end of the fiber is illuminated, to help focusing procedures, one of the critical points of this technique. Considering that a very small spot is need in order to have good spatial resolution and also a high numerical aperture beam to get around the leaky rays problem, focusing is very difficult. The depth of focus is given by $\lambda/2\sin^2\theta_{i\,max}$ so for a 0.5 NA we have a 2 microns tolerance in the focusing of the fiber. This imposes a very good quality end face

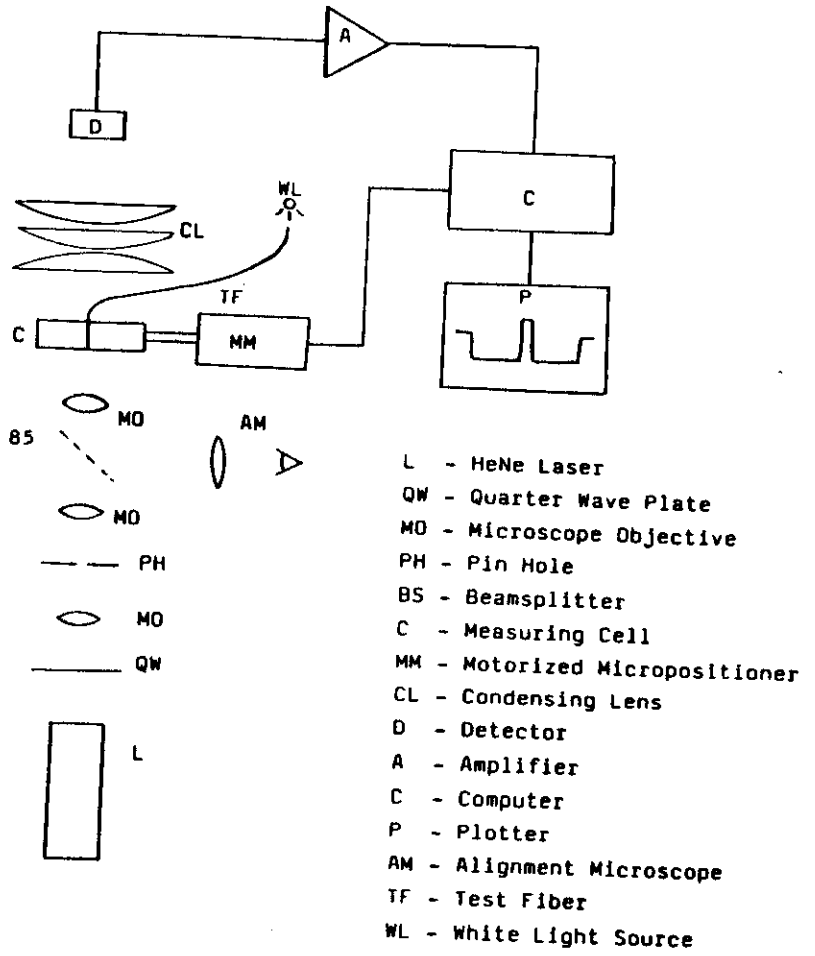

Fig. 10 - Experimental set-up for measuring index of refraction profile by the refracted near field method.

preparation and a very good alignment with respect to the focusing plane.

Typical results using the refracted near field technique is shown in Figure 11, for both multimode and monomode fibers. Note that by using careful calibration procedures, the absolute value is obt. It is claimed that a index variation of less than 1×10^{-5} can be detected. Nowadays, this method of measuring the index of refraction profile of optical fiber is the most popular one and various other set-ups, based on the same principles, are being used, even in commercial equipments.

3.4. TRANSVERSE INTERFEROMETRIC METHOD

One technique, that has been used in our laboratory extensively for many years, is based in complete different concept than the one just discussed. Because is an absolute measurement and do not rely on any guidance property of the fiber, is worthwhile to describe it.

Since the index of refraction variation of the fiber is very small, a plane wave propagating perpendicular to the fiber, immersed in a liquid with the same index of refraction of the cladding can be considered, to experience only a phase shift, proportional to the index difference. If this wave, is then combined with a reference plane wavefront, it will produce an interference pattern that will contain the information about the transversed medium. Let us refer to Figure 12 to calculate the optical path difference.

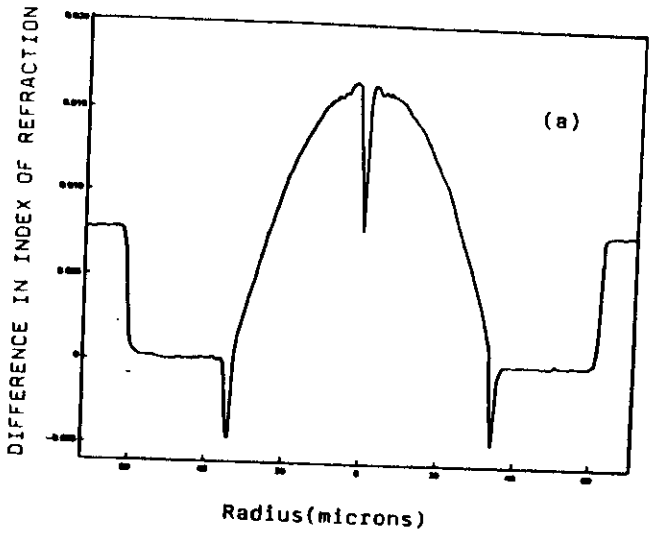

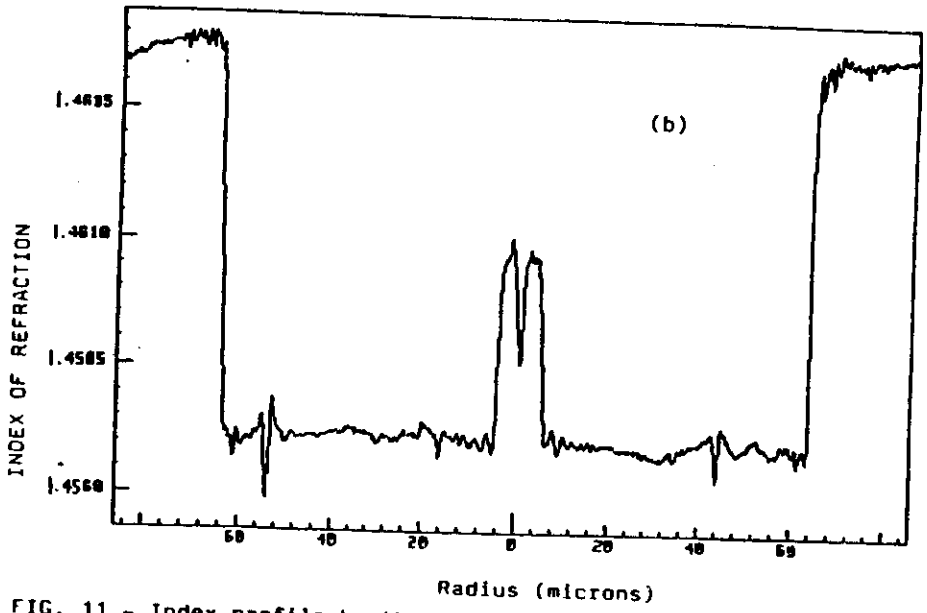

FIG. 11 - Index profile by the refracted near field method
a) multimode fiber (from K.White, Opt.Quant.Electr.11 (1979), 18
b) monomode fiber (courtesy from J.P.Pellaux)

$$OPD(r) = \int_{-h}^{h} (n(s) - n_o)\, ds \qquad (20)$$

since $s^2 = \varrho^2 - r^2$ and $n(r) - n_o = o$ for $r>a$ then (20) can be transformed to

$$OPD(r) = 2\int_{r}^{\infty} \frac{(n(\varrho) - n_o)}{(\varrho^2 - r^2)^{1/2}}\, \varrho\, d\varrho \qquad (21)$$

Interfering the output wavefront with a paralell wavefront, will produce an interferogram as shown in the inset of Figure 12. The fringe shift S(r) is given by

$$S(r) = \frac{OPD(r)\ .\ Q}{\lambda} \qquad (22)$$

where Q is fringe spacing in the undistorted region.

Equation (21) can be inverted, using what is called Abel transformation (Marcuse relation), so the index difference is written as

$$\Delta n(\varrho) = -\frac{\lambda}{\pi Q} \int_{\varrho}^{\infty} \frac{dS(r)}{dr} \frac{dr}{(r^2 - \varrho^2)^{1/2}} \qquad (23)$$

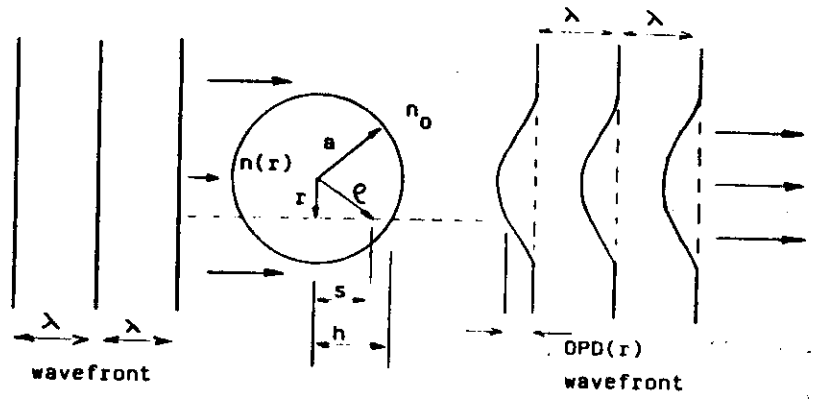

(a)

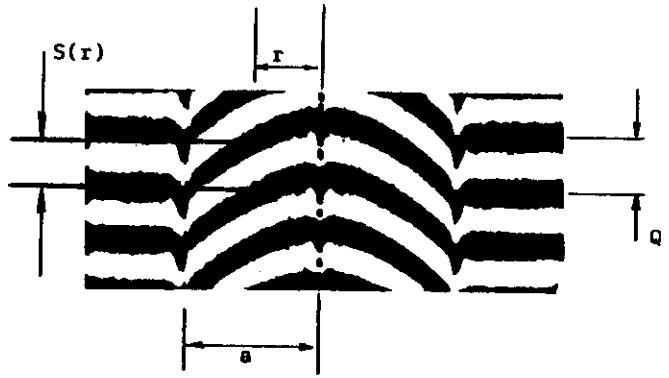

(b)

FIG. 12 - a) Transverse interferometric technique for measuring index profile: basic geometry.
b) Mesured interferogram.

Thus by measuring the fringe shift function S(r), Eq (23) may be solved, yielding the desired index profile. Because of the geometry used, it is assumed that the fiber has circular symmetry and this may not be the case sometimes. Nevertheless, since this method doesn't depend on any guidance property and provides an absolute measurement, without any complicated calibration and focusing procedures, it is very attractive.

For the practical implementation of the method just described we used a Mach Zender interference microscope as shown in Figure 13. To obtain good fringe visibility a monochromatic light source is used. The fringe pattern is analyzed with a TV camera coupled to a microcomputer in order to perform the calculation given by Eq. (23). In Figure 14 we show the results obtained with the present technique in multimode and monomode fibers. Since in Eq. (23) the derivative of the fringe shift is involved, this method is very sensitive to structures that appear in index profile. Also, because the integrand diverges at the center of the fiber, the measurements errors increase very fast near the axis. In any case, outside this region, the precision, for circular fibers is better than 0.0005. For elliptical core fibers, there are ways of making dependable measurements, at the cost of orienting the fiber properly in the microscope and changing slightly the basic Eq. (23).

3.5. PREFORM INDEX OF REFRACTION MEASUREMENTS

Most of the index of refraction information of fibers is

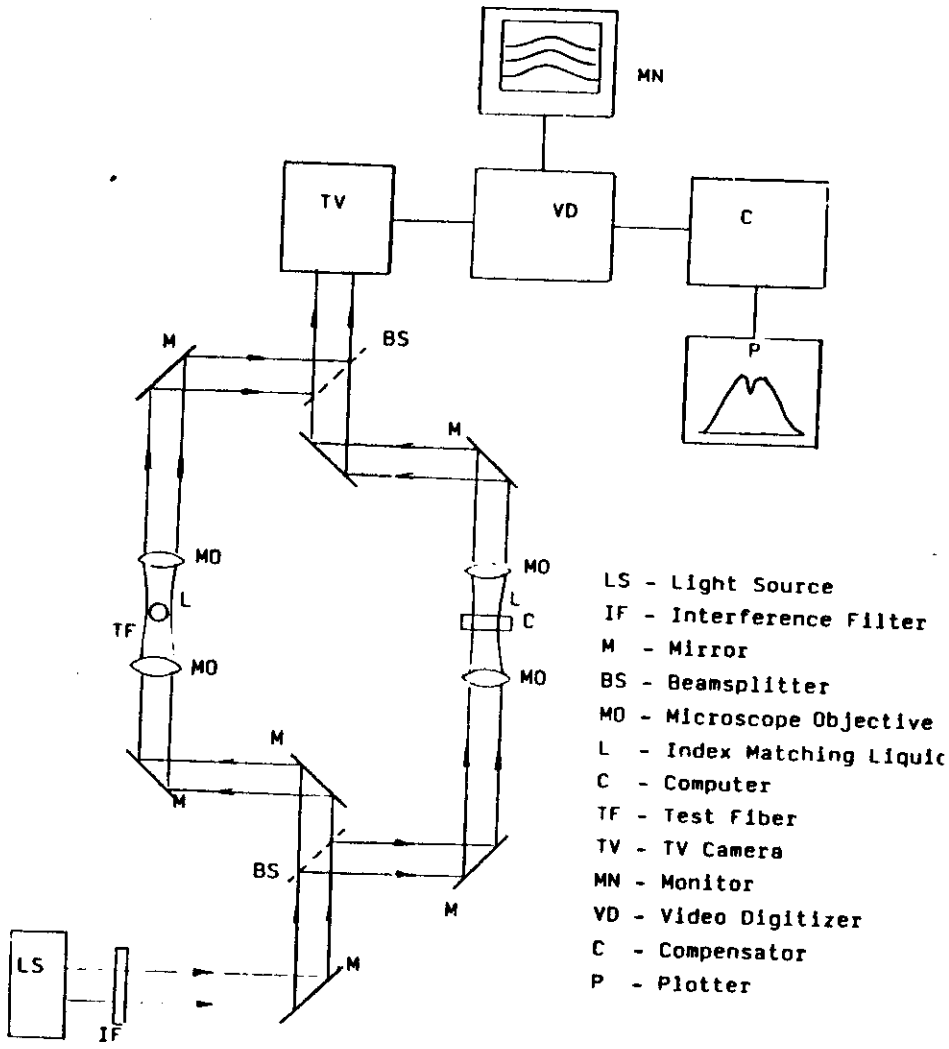

FIG. 13 - Mach-Zehnder interference microscope schematic and image processing equipment for measuring the index of refraction of optical fibers.

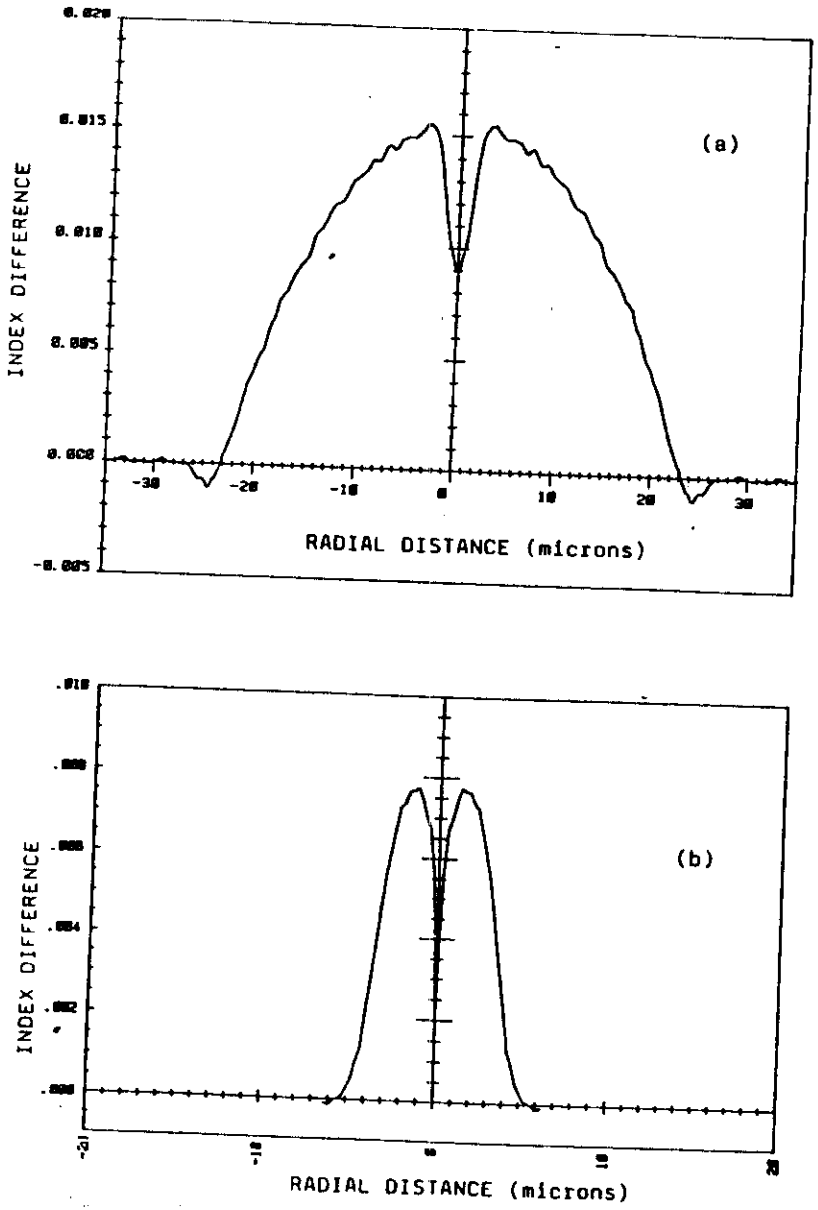

FIG. 14 - Index of refraction profiles by the transverse interferometric method. (a) Multimode and (b) Monomode.

already available in the preform. The geometrical dimensions involved now, is at least 100 times larger than in the fiber, making measurements easier in this aspect. The question whether, the index profile in the preform and fiber are exactly the same, is raised sometimes due to the fiber drawing process and the difficulties inherent in the measurement process. It is our experience, that the preform index of refraction profile information can be used as a controlling parameter to optimize the fiber fabrication in regard to glass deposition rate and bandwidth in the case of multimode fibers. For monomode fibers, were the core's spatial dimensions are even smaller, the preform's profile is very valuable in controlling parameters, such as cut-off wavelength mode field diameter and dispersion properties, apart from allowing the design of fibers, for a low loss performance.

Because of the preform dimensions, we can not use any of the profiling methods discussed so far. The most used technique, consist of measuring the deflection angle of a light ray that passes perpendicular to the preform axis, as shown in Figure 15.

The deflection angle Θ is related to the index of refraction distribution n(r) and the ray position t by the following equation

$$\tan\Theta = \frac{2t}{n_o}\int_t^a \frac{\partial n(r)}{\partial r}\,\frac{dr}{(r^2 - t^2)^{1/2}} \qquad (24)$$

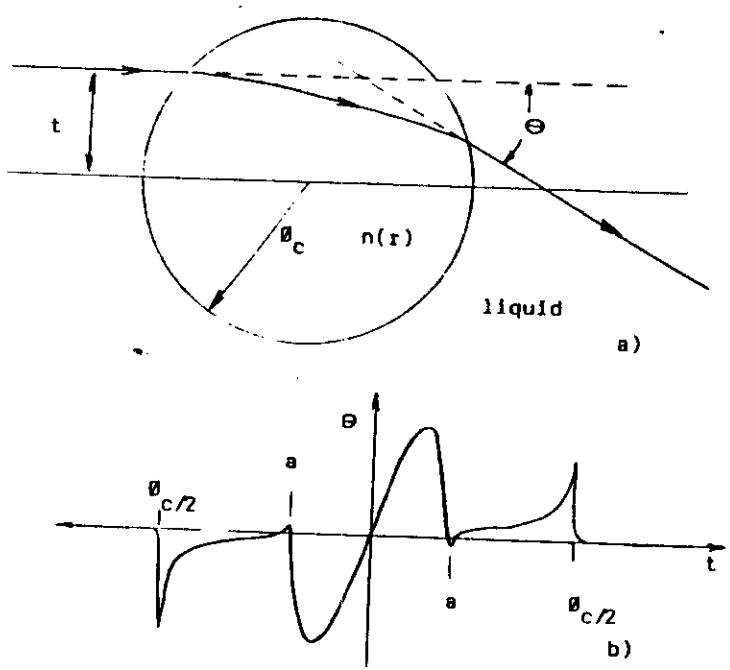

Fig. 15 - a) Basic geometry for measuring index of refraction by the refraction method.
b) Deflection function Θ for a graded index fiber.

Just as the transformation,between Eqs. (21) and (23) we can transform Eq. (24) to

$$\Delta n(r) = -\frac{n_o}{\pi}\int_r^{\infty} \frac{\tan\Theta}{(t^2-r^2)^{1/2}}\,dt \qquad (25)$$

Again, as in section 3.4, circular geometry is assumed.

Nowadays, there are commercial equipments that measures the index profile,based on the principle just described. The preform is immersed in a cell with a liquid that is near the same index of refraction as of pure silica, to avoid problems of outer surface quality and to improve measurement precision. The whole cell is then scanned past the light beam and the deflection function $\Theta(t)$ measured. In a second step, calculation using Eq. (25) gives the index profile. Examples of the results for multimode and monomode preforms are shown in Figure 16. Profile scanning cab be performed at various points along the preform so as to characterize for example, how uniform is the index of refraction down the length. In Figure 17 we can see five profile in the first 23 cm of a preform. It is obvious in this figure, that a diameter variation is occuring, thus giving valuable information on the preform fabrication process as well as showing that the first 10cm must be discarded in order to obtain a uniform fiber.

3.6. INDEX OF REFRACTION DATA ANALYSIS

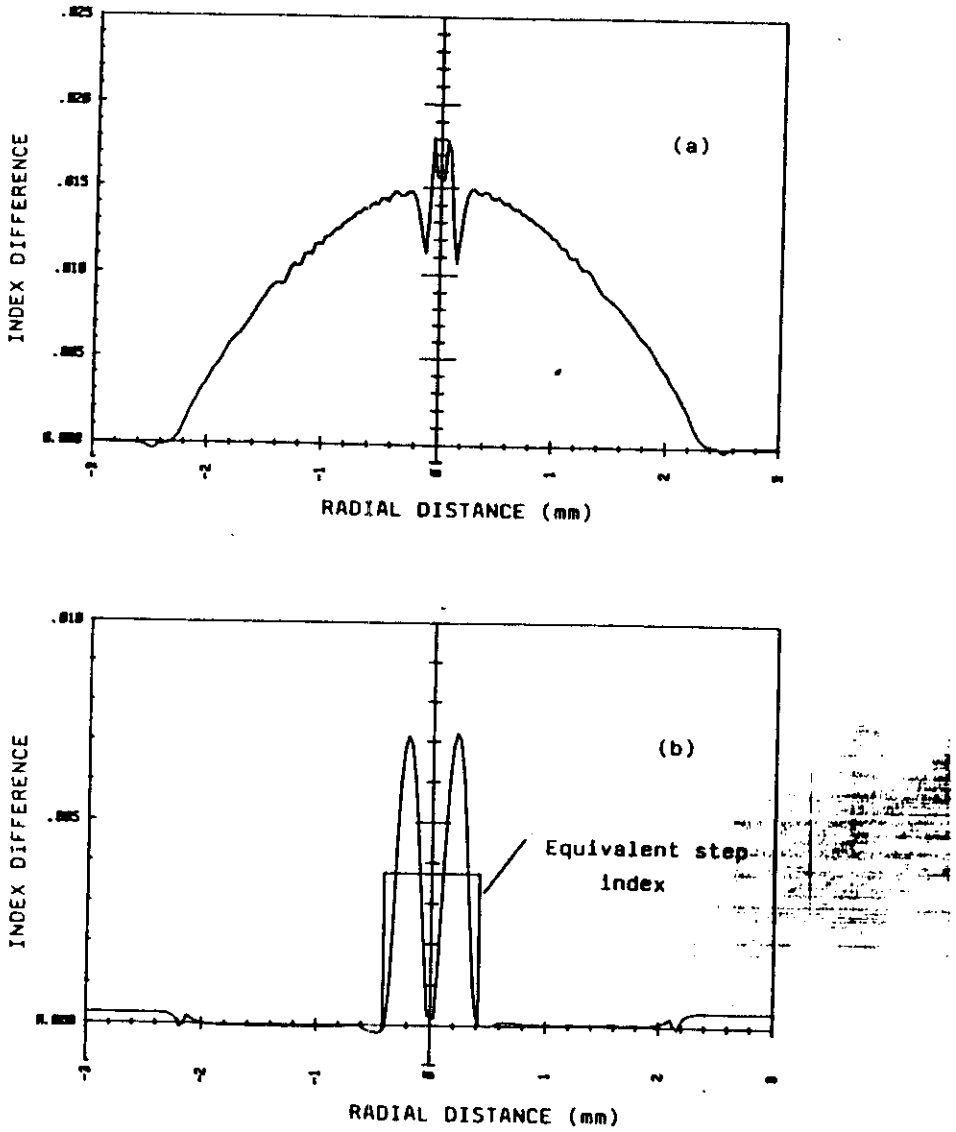

FIG. 16 - Index of refraction profiles from:
(a) multimode graded index preform
(b) monomode matched clad preform.

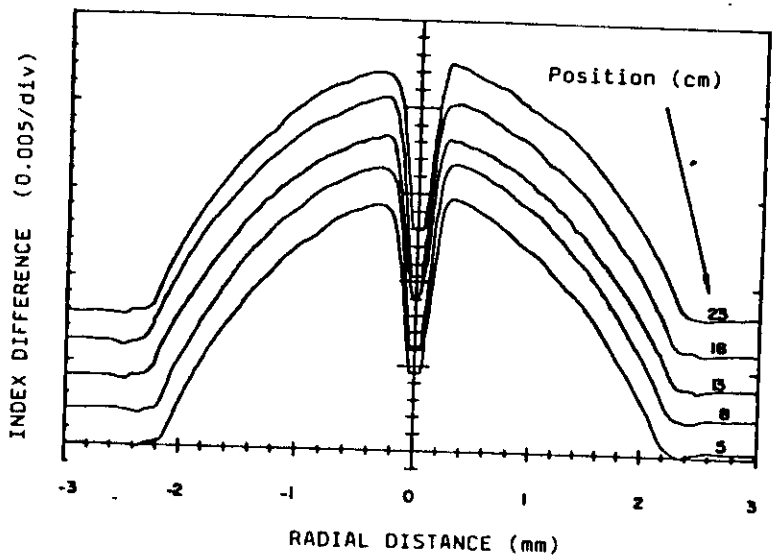

FIG. 17 - Index of refraction profiles along the preform length.

Once the index profile is obtained in the fiber or preform,relevant parameters must be extracted from it and correlated with other results such as bandwidth and numerical aperture results in multimode fiber. For monomode fibers, parameters as cut -off wavelength, mode field diameter, chromatic dispersion can be calculated from the preform index profile and correlated with the experimental results.

A convenient way of describing the index of refraction profiles of graded index fibers or preforms in terms of few parameters is fitting it, with the following mathematical expression

$$n(r) = n(o)\left[1 - \Delta(r/a)^{\alpha}\right] \qquad (26)$$

for r equal or smaller than the fiber core radius a. This is the so called α, Δ profile for which extensively calculation has been done, in relation to fiber transmission properties.

Another important parameter, the deviation of the measured profile from Eq. (26), can be defined as,

$$\chi^2 = \sum_{i=1}^{N} \frac{\left[n(r) - n_c(r)\right]^2}{N} \qquad (27)$$

where n(r) is the measured index and n_c the one calculated by Eq. (26).

Optimum fiber performance is obtained when α nearly 2 but this value can be slightly modified, depending on wavelength and dopants used in the fabrication process. The lack of defects in the profile as given by small χ values, is also relevant in terms of bandwidth. Just to illustrate this point, in Figure 18 is plotted the fiber bandwidth as a function of χ for two family of α values. It is obvious that correlation exists for both cases, especially in the higher leftside of the plot, representing top quality fibers.

Finally, correlations can also be made on profiles measured in fibers and preforms. If we use the α , Δ and χ parameters as describing the profiles, and use them for comparison we have the results shown in Table 3. The fibers were measured using transverse interferometry techniques and the preforms with a York Technology equipment employing the method described in the section 3.5

TABLE 3

FIBER-PREFORMS PROFILE COMPARISON*

PARAMETER	AVERAGE ± STANDARD DEVIATION
$\alpha_{pref}/\alpha_{fiber}$	1.03 ± 0.08
$\Delta_{pref}/\Delta_{fiber}$	1.008 ± 0.042
χ_{pref}/χ_{fiber}	0.8 ± 0.2

* based on 15 profiles

By these results we tend to see that the agreement is quite good. The higher value of χ_{fiber} is probably related to the high sensitivity of the interferometric technique for detecting profile imperfections.

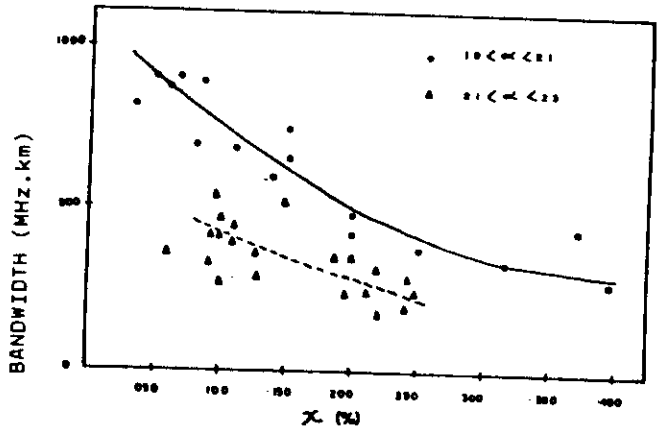

FIG. 18 - Fiber bandwidth as a function of index of refraction profile α, χ parameters.

4. FIBER LOSS MEASUREMENT

4.1. INTRODUCTION

The fiber loss along with the available bandwidth are the two most important parameters for a fiber user. The knowledge of fiber attenuation will permit the designing of an optical system in terms of repeater spacing, splicing, power margin and signal to noise ratio or error rate in the detection, for a given input power. For a fiber loss measurement to be useful, it must give a value that represents an equilibrium situation in terms of power distribution among the various propagating modes in case of multimode fiber. If a worst case value is adopted,we may incur in problems of overspecifying the fiber thus running into cost problems. On the other hand, restricting the mode excitation, there can be an exclusion of other higher loss modes that may participated in a real system, causing then, receiver power penalties. These types of problems can be even worst if we take into account that fibers with different index profiles, primary coating, cabling and lay out conditions can behave in distinct ways. Specially for low loss multimode fibers in the 1.3 microns region, where every fraction of a dB/km counts, loss measurements conditions must be controlled very well. In the case of monomode fibers, the situation is much easier with respect to all those problems.

There are basically two ways of measuring fiber loss, that are been employed almost everywhere. The first one consists of launching a certain amount of power into a fiber and then measuring the signal level in two well separated points along the

fiber. In this manner, the loss in a certain length is determined and this value is usually normalized in terms of dB/km. Since the light source wavelength can be easily varied, a spectral loss curve, is obtained, which is very useful for fiber performance and fabrication process analysis. The other technique, that is not destructive, a short laser pulse is injected into the fiber and the backscattered signal is observed as a function of time. In this way, the power intensity along the fiber length is measured, permitting the extraction of informations concerning fiber homogeneity, splice loss, localized faults, fiber length, local attenuation and end to end loss. This type of measuring technique is ideally suited for the fiber user preocupied with cabling, laying out and splicing fiber cables. But even in the laboratory, this measuring method gives informations that are necessary for fiber development and fabrication.

In the sections that follow, we should go into the details of these two techniques.But before that, the basic loss mechanism in fibers will be briefly reviewed for a better appreciation of the measuring methods and results.

4.2. LOSS MECHANISM IN OPTICAL FIBERS

There are several loss mechanisms that can attenuate a light signal propagating in an optical fiber. They can be divided in two classes, absorption and scattering and this last one in intrinsic and extrinsic factors. The pure silica glass absorption mechanisms are atomic absorption in the ultraviolet region and molecular absorption in the infrared and they are both very small

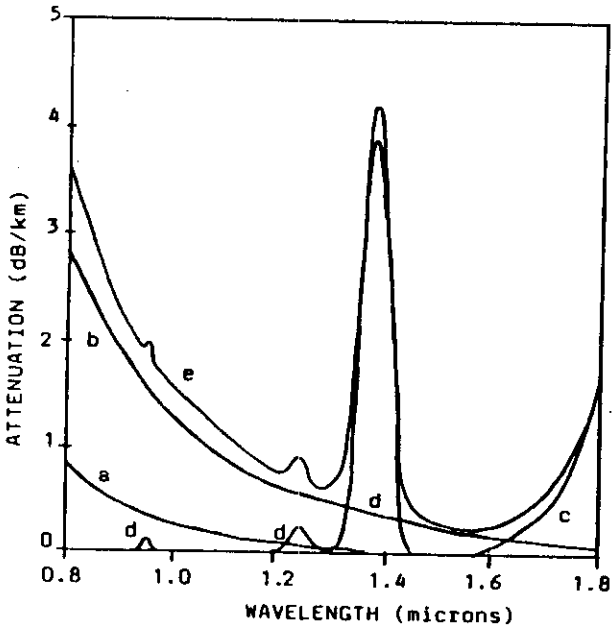

FIG. 19 - Basic loss mechanism in optical fibers. (a) UV absorption;(b) Rayleigh scattering;(c)IR absorption; (d)OH absorption (0.1ppm) and (e) total loss (a+b+c+d).

in the region of interest, between 0.8 and 1.5 microns. Dependent on the glass dopants being employed, there can be a presence of infrared molecular absorption near 1.5 microns specially for boron or high concentration of phosphorus. Another cause of absorption is the presence of contaminants in the form of transition metals and more important of OH radical. The first ones are completely eliminated with high quality starting materials and the second ones depend on processing techniques and are always present in MCVD fibers, even though its influence on the attenuation at the operating wavelength are been kept very low today. The other intrinsic loss factor is the Rayleigh scattering that depends on the type of glass micro structure and dopants used and represent the theoretical loss limit in any kind of fiber.

In terms of extrinsic scattering factors we have in multimode fibers,waveguide imperfections induced loss and cabling effects, when the outer coatings deform the fiber and in both cases we don't expect a very strong wavelength dependence. But in monomode fibers, these external induced microbendings produce a very rapidly increase in loss as a function of wavelength and it is also dependent on the index of refraction profile. All of the above loss mechanisms are shown graphically in Figure 19. As will be discussed later, an experimental spectral loss curve can be decomposed in some the components just described and give valuable insight into the fiber fabrication process.

4.3. CUT-BACK TECHNIQUE

If we have light propagating inside the fiber, the amount of absorbed and scattered light in a given length dz of fiber is

$$dP = -\left(\alpha'_A(z) + \alpha'_s(z)\right) P\, dz \qquad (28)$$

where the α's are the absorption and scattering coefficients and P the intensity at point z. Integrating (28) we have

$$P(z) = P_o\, e^{-\int_o^z \alpha'(z)dz} \qquad (29)$$

where P_o is the intensity at point z=0. For a homogeneous fiber, the integral reduces to

$$P(z) = P_o\, e^{-\alpha'_A z} = P_o\, 10^{-\alpha z/10} \qquad (30)$$

The most common and reliable way of determining fiber loss is to insert a given optical power in one end of the fiber and measure the light intensity at the other end. The next step is to cut the fiber near the launching end and measure the intensity again without disturbing the input end conditions.

The loss is then given immediately by

$$\alpha(\lambda) = \frac{-10 \log \left[\dfrac{P(z_1)}{P(z_2)}\right]}{(z_1 - z_2)} \text{ dB/km} \qquad (31)$$

where $P(z_1)$ and $P(z_2)$ are the intensities measured at point z_1 and z_2 respectively. The input P_o power can remain unknown, provided is the same in both measurements.

If a non equilibrium mode configuration is excited, the higher order modes (that have a higher loss) will die off before the others, thus changing the mode distribution. In this case, the effective loss coefficient, defined as

$$\alpha_{eff}(z) = \frac{\sum \alpha_i P_i}{\sum P_i} \qquad (32)$$

where α_i and P_i are the loss and power in mode i respectively, will change along the fiber. In this situation, the measured attenuation defined by Eq. (31) will depend on the fiber length as well on the power distribution (P_i) among the modes. Because of this extreme care must be taken to ensure that:1) no unwanted modes should be launched; 2) an equilibrium mode distribution must be obtained before the point where the second measurement (shorter length fiber) is made.

The basic experimental set-up to implement the cut-back method is shown in Figure 20. The light source must emit a reasonable flat spectrum in the region of interest, and a tungsten quartz halogen filament lamp is quite adequate from 0.5 up to almost the 2 microns region. The monochromator or a set of interference filters can select the appropriate wavelength and a 10nm spectral width is good enough. An optical system consisting

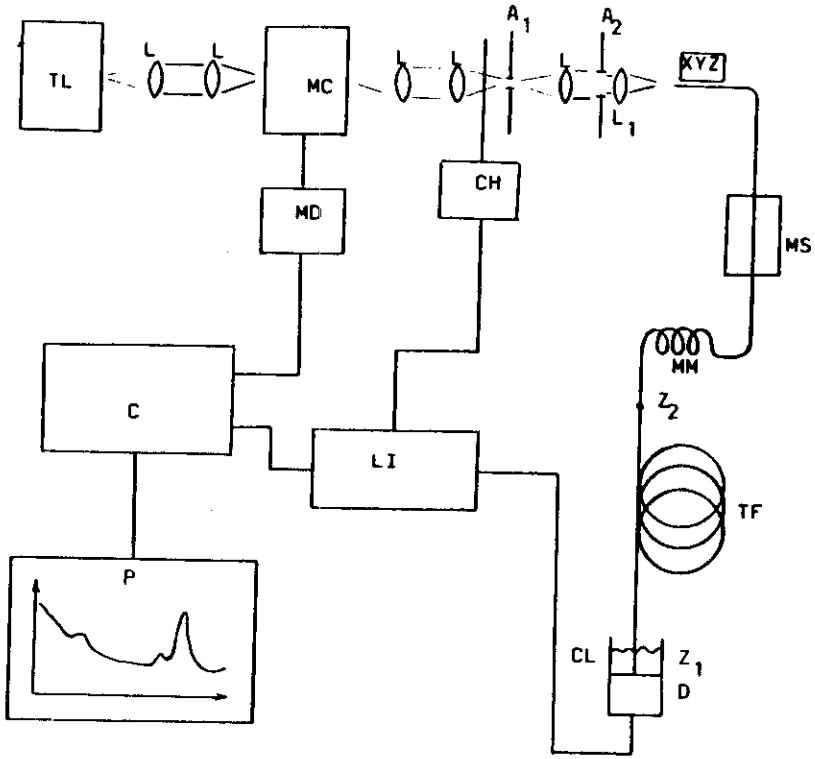

TL - Tungsten Lamp
L - Lens
MC - Monochromator
MD - Monochromator Driver
CH - Chopper
C - Computer
LI - Lock-in Amplifier
P - Plotter
XYZ- Micropositioner

A_1 - Spot size aperture
A_2 - NA Aperture
L_1 - Microscope Objective 20x
MS - Mode Stripper
MM - Mode Mixer
TF - Test Fiber Reel
CL - Coupling Liquid
D - Detector

Fig. 20 - Experimental set-up for measuring the spectral loss curve by the cut-back method.

of three lenses and two apertures will produce an image in the face of the fiber with controlable spot size and numerical aperture. The fiber is positioned in front of the last microscope objective with a three degree of freedom micropositioner. The fiber face must be carefully prepared to increase the light coupling. For fibers that have a low index of refraction primary coating such as silicone, a cladding mode stripper is used to remove this unwanted modes. Immersion of few centimeters of the fibers, without the coating in glicerol is sufficient. The procedure to reach an equilibrium mode distribution can be wrapping a few turns of the fiber around a 1 cm rod. The optimization of the launching conditions and of the mode filter can be done in the following way. Excite the fiber with a light beam having a spot size and numerical aperture at least the same as the fiber's core. Without the mode filter, measure the far field angle (see section 3.2) of a full length fiber. Cut the fiber at the reference length z_2, introduce the mode filter between the last microscope objective and the fiber, and adjust the mode filter until the same far field angle as in the first step is obtained.

For repeatable measurements, the fiber must not be very tightly wrapped (a 50 grams tension is usually employed in the reel). The coupling of the fiber end with the detector must be very reproducible and the use of a coupling agent such as a liquid, can be employed. A large area detector with a good response in the region of interest is used. For measurements from 0.5 to 1.0 microns a silicon detector is the choice. For

wavelenghts above that, a cooled germanium or PbS detectors can be employed.

Since the measured signals are very small, an AC detection scheme, using a light chopper and a lock-in amplifier is used. Normally a microcomputer is used for storing measured data and controlling the monochromator driver and lock-in amplifier. At each wavelength several measurements are performed, the number depending on the signal to noise ratio. For the second measurement, the fiber is cleaved at the point z_2 (a reference length about 2.5 meters is normally used) and all the data taking procedures repeated without disturbing the launching end.

For monomode fibers, a mode filter is not necessary unless we want to filter out the higher order modes and measure only the fundamental mode loss in a region near and bellow the cut off point. It has been our experience that the coupling reproducibility between the fiber and the detector can be improved if is done via a multimode fiber. This is probably due to the fact that detector sensitivity varies along the detection surface, and a multimode fiber illuminates a much larger area than a monomode, thus averaging out any non-uniformity.

Typical measurements results are shown in Figure 21 for both types of fibers. The measurement precision is about 0.1 dB/km and 0.05 dB/km for multimode and monomode fibers respectively. Of course, measuring long length fibers gives better precision because of the larger differences in the measured signals.

From the attenuation curves shown in Figure 21, a serie of informations concerning the basic loss mechanism can be extracted.

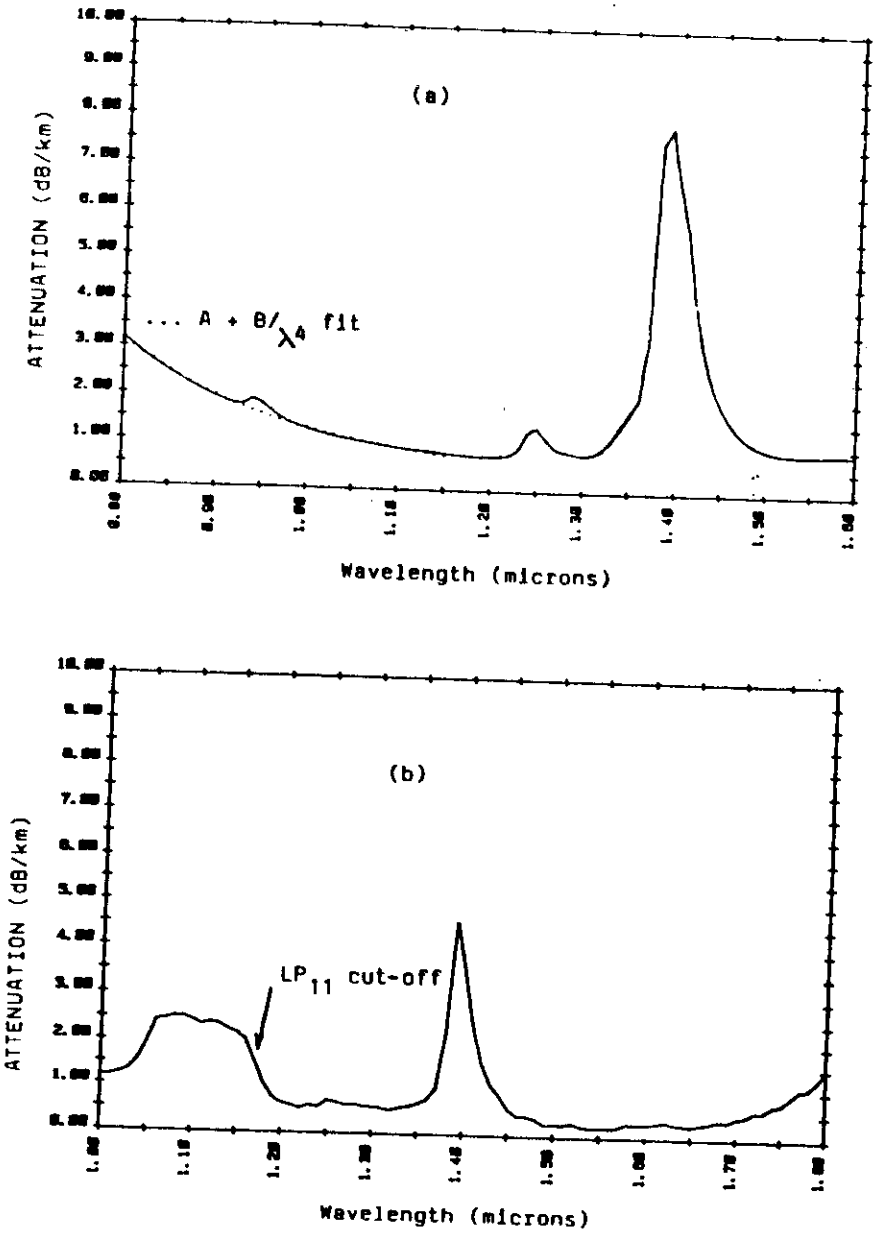

FIG. 21 - Attenuation curves for:(a) multimode graded index and (b) monomode.

Recording that the Rayleigh scattering, waveguide imperfections and OH contamination are the three more important loss factors, in the region between 0.8 and 1.6 microns, the loss curve can be described by

$$\alpha(\lambda) = A + B/\lambda^4 + C(\lambda) \qquad (33)$$

The A parameter is related mostly to waveguide defects induced loss and microbendings. B is the Rayleigh scattering parameter and C is associated with the other mechanisms such as absorption due to OH content. Fitting the experimental curve in the region from 0.8 to 1.2 microns, with this expression can give the loss parameters. A practical way of doing this is to plot the loss curve in a $1/\lambda^4$ scale, thus producing a straight line in the region where $C(\lambda)$ is zero. For general multimode fibers, A is of the order of 0.4 dB/km and $B \sim 1.2$ dB/km.μm^4. The value of C_{OH} (.95 μm) related to the water content, is about 1 dB/km.ppm of OH. In the other wavelengths of interest, C_{OH} (.85 μm) = 0 and C (1.3 μm) = C (.95), so the excess loss in this important wavelength (1.3 um) is greatly influenced by water in the fiber.

4.4. BACKSCATTERING TECHNIQUE

As seen in section 4.2, one of the basic loss mechanism is the Rayleigh scattering, that scatters light isotrophically in all directions. This effect can be used for measuring fiber attenuation by observing the backscattered light.

Illuminating the fiber from one end, the optical power at a given point z, is given by Eq. (29). The amount of power reflected back and guided in the fiber is then RP(z) where R is the reflection coefficient. So, the received power at the input end, reflected from z, is

$$P_s(z) = RP_o \cdot e^{-\int_0^z \alpha'_F dz} \cdot e^{-\int_0^z \alpha'_B dz} \qquad (34)$$

where α'_F and α'_B are the loss coefficient in the forward and backward direction respectively. They can be different because of the different lauching conditions in the two directions . If the injected light is in the form of a narrow pulse, emitted at time t=0, then the observation of the backscattered pulse intensities at time t correspond to the reflected light from point $z = tv_g/2$, where v_g is the group velocity.

Using Eqs. (33) and (30) the local loss coefficient is given by

$$\alpha_F(z) + \alpha_B(z) = \frac{d}{dz}\left[10 \log P_s(z)\right] \qquad (35)$$

or

$$\alpha_F(z) + \alpha_B(z) = \frac{2}{v_g} \frac{d}{dt}\left[10 \log P_s(t)\right] \qquad (36)$$

In other words, the fiber loss can be measured by observing the pulse shape of the backscattered light. When a uniform attenuation and same forward and backard loss coefficient is assumed, the fiber loss is simply

$$\alpha = 5.\log\left[P(t_1)/P(t_2)\right] \Big/ \left[\frac{(t_2 - t_1)v_g}{2}\right] \qquad (37)$$

where $P(t_1)$ and $P(t_2)$ are the pulse height at times t_1 and t_2.

In Figure 22 is shown an experimental set-up for measuring fiber loss according to this technique. A sharp light pulse from a semiconductor laser is launched in the fiber via an optical fiber coupler, or a beamsplitter. The backscattered light is direct by the coupler to a fast detector. Because of the low light level, a box-car averager for signal processing is necessary. In the figure, is also shown the pulse shape. One can see the typical exponential form given by Eq. (34) and the two points used for calculation of the loss with Eq. (37). The signature for a splice between the two test fibers is illustrated. The loss at this point is determined by knowing that the detected light from just before the splice is $P_1 = P_s(z)$ and after $P_2 = P_s(z).K_f$ where K_f and K_b are the loss coefficient for

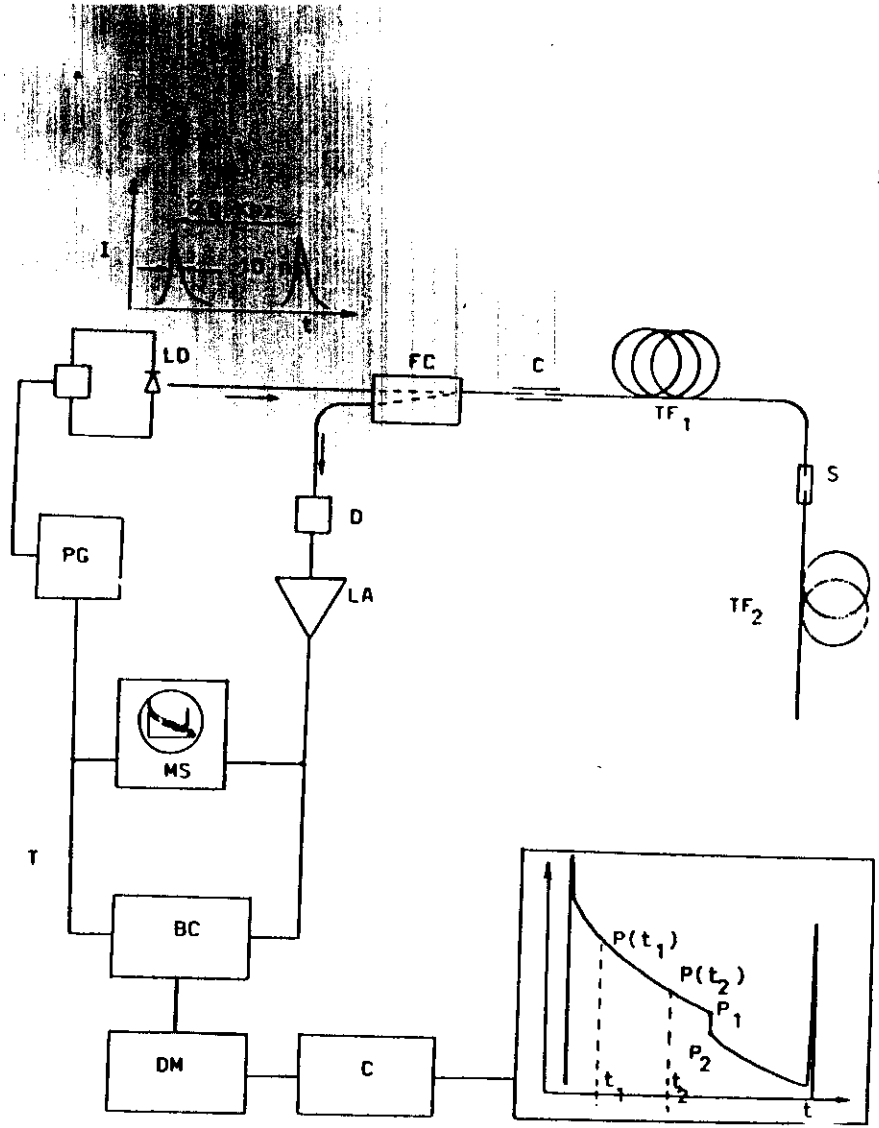

LD - Laser Diode
PG - Pulse Generator
LA - Low Noise Amplifier
MS - Monitor Oscilloscope
BC - Box-Car Averager
T - Trigger
C - Connector
D - Detector
LA - Low Noise Amp.
DM - Digital Memory
C - Coupler
P - Plotter
$TF_{1,2}$ - Test Fibers
S - Splice
FC - Fiber Coupler

FIG. 22 - Optical Time Domain Reflectometer for fiber measurements.

going through the splice in the forward and backward direction. If the two are the same, the splice loss (K) is simple

$$K = 5 \log (p_1/p_2) \quad dB \tag{38}$$

For the determination of the fiber loss, we can use Eq.(36) when the fiber is homogeneous or when we want to know the average loss over a given region. Two measurements are done by injecting light from one and from the other end of the fiber and then taking the average between them. If the local attenuation over the fiber is needed, the derivative of the curve is used, according to Eq. (35). In both types of analysis, what is normally done is to plot the backscattered curve in a log scale directly in dB's. In Figure 23 experimental data, from graded index fiber is shown, where all the above procedures are illustrated.

As mentioned before, the position along the fiber of any point in the backscattered pulse shape is

$$z = \frac{t}{2} \cdot v_g \tag{39}$$

The group velocity of the light inside the fiber is

$$v_g = \frac{c}{N} = \frac{c}{\left[n(\lambda) - \lambda \frac{dn}{d\lambda} \right]} \tag{40}$$

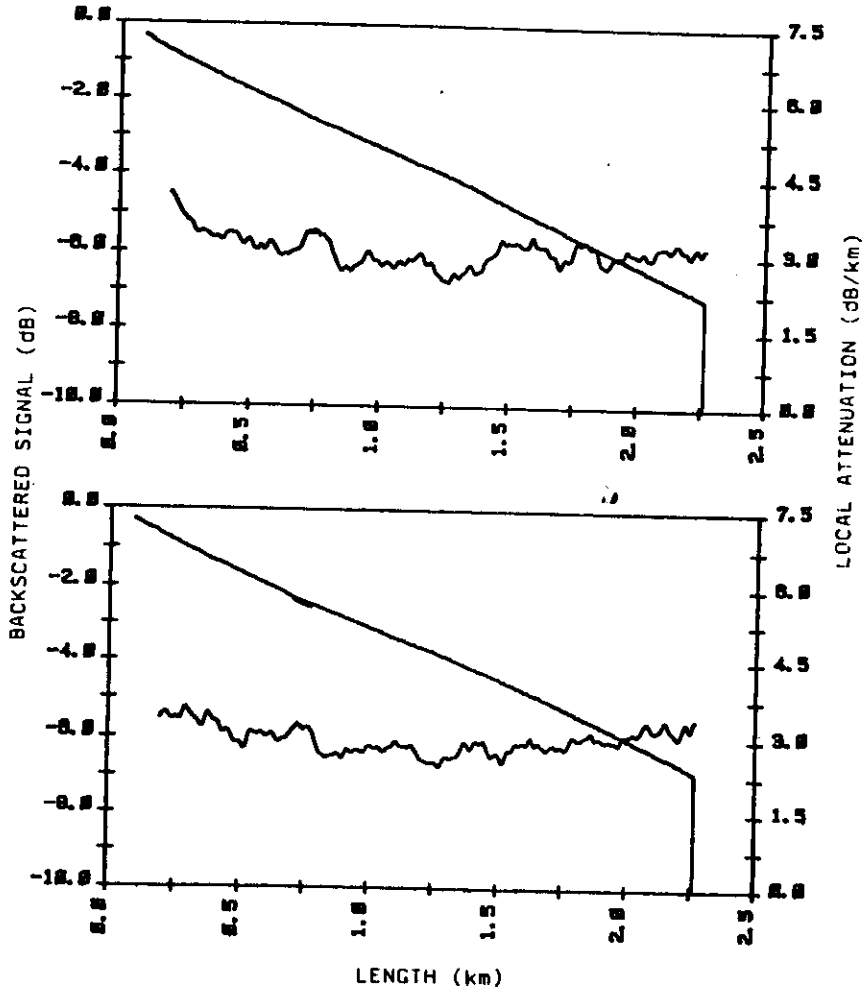

FIG. 23 - Loss measurement by the optical time domain reflectometry technique. Data taken from both fiber ends.

where c is the velocity of light in vacuum and n the fiber index of the refraction at the given wavelength. The group index N varies as a function of wavelength and core's material constituents, as shown in Table 4.

TABLE 4

GROUP INDEX FOR VARIOUS GLASSES

Wavelength (microns)	Silica		13.5 GeO_2 + 86.5 SiO_2	
	n	N	n	N
0.85	1.453	1.467	1.474	1.488
1.30	1.447	1.461	1.469	1.481
1.55	1.445	1.463	1.466	1.481

These data can be used to calculate the fiber total length. In Figure 22 the far right peak is due to the reflection at the fiber-air interface at the end of the two spliced fibers. The precision by which the fiber length or any other feature in the backscattered signal can be measured is a function of pulse width and the proper knowledge of the effective group index parameter, that the light really sees. Assuming that the time resolution is that given by the pulse width (σ), the spatial

resolution is then

$$\Delta z = \frac{c}{N} \cdot \sigma \qquad (41)$$

Since normally a 10 ns pulse is used, $\Delta z \sim 2$ meters. Considering that the group index is known to within 0.5%, this will add to the other error just mentioned.

The backscattering technique described, is being widely used nowadays for multimode and monomode fibers. Portable commercial instruments with all kind of sophisticated signal and data processing is available. The advantages of the method, of being non destructive, using only one end of the fiber and producing a large number of information about fibers and splices make it very attractive. Because of the different mode excitation with respect to that used in standard cut back techniques, small differences in the attenuation values are expected. In Figure 24 these differences are plotted for the case of graded index multimode fibers. The cut back technique gives a smaller value, than the backscattering technique, the difference being around 0.1 to0.2 dB/km.

This difference is due to the high order mode excitation which occurs with the backscattered light which is isotropic as compared to the restricted launching used in the cut-back method.

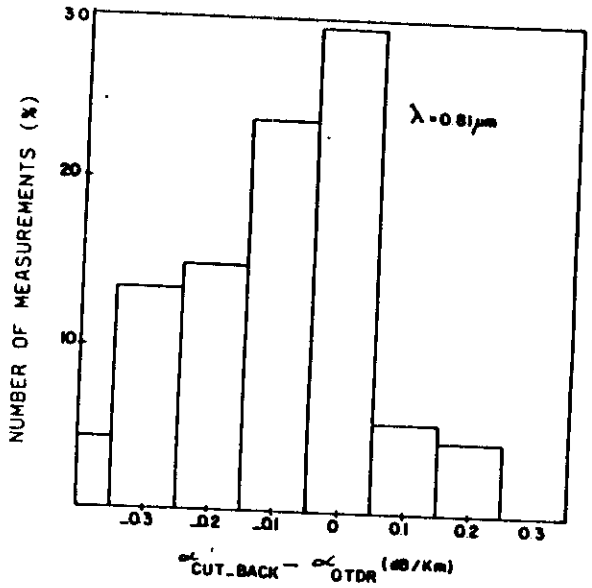

FIG. 24 - Histogram of difference in measured loss values between the cut-back and optical time domain reflectometer (OTDR).

5. FIBER BANDWIDTH MEASUREMENT

5.1. INTRODUCTION

Together with the overall carrier attenuation, the available modulation frequency bandwidth are the two important characteristics in a fiber optic transmission line. In this section we would describe the basic techniques used in measuring the fiber properties that may affect the information carrying capacity.

As it is well known, time and frequency response, of a linear system, are related to each other by a Fourier transformation. But even though, bandwidth measurements techniques in multimode fibers are divided in time domain methods in which the temporal characteristics of a pulse shape is measured and frequency domain, where the attenuation of each frequency component is determined.

The physical mechanism, responsible for the bandwidth limitation is the time broadening of the light pulses when it travels down in the fiber. When the pulse power is carried by many modes as in the case of a multimode fiber,the different transit times of each mode accounts for the time broadening of those pulses.When the pulse power is carried by only one mode, as in a monomode fiber, the spectral components of the pulsed optical source travel with different group velocity causing a time broadening.

Formally, the transit time (τ) of a pulse signal over a distance L is

$$\tau_i = \frac{L}{v_g} = L \frac{d\beta_i}{dw} \qquad (42)$$

where β_i is the propagation constant of mode i and w the optical frequency. The difference in transit time between two spectral components separated by $\delta\lambda$ is

$$\delta\tau_i = \left(\frac{\partial\tau_i}{\partial\lambda}\right).\delta\lambda \qquad (43)$$

where the derivative can be shown to be

$$\frac{\partial\tau_i}{\partial\lambda} = -\frac{\lambda L}{c}\frac{d^2 n_o}{d\lambda^2} + L \cdot T(\lambda,\beta) \qquad (44)$$

where the first term is the so called material dispersion and the second one the waveguide dispersion. This last one depend on the fiber index of refraction profile and in some circunstances can be made exactly the opposite to the material dispersion, for certain wavelengths, thus yielding a fiber with nc intramodal broadening. This artifice is used very often in monomode fiber design.

In a multimode fiber, for every mode there is a particular transit time τ_i. So to calculate the total broadening one needs know the number of modes excited and the amount of power in each one

and them sum up all the contributions. Chromatic dispersion given by Eq. (43) must be added for every mode if the light source is not monochromatic. This is a very complicated calculation and the result depend strongly on the fiber index of refraction profile.

Assuming that the fiber has an index profile given by Eq. (26), and also, that all guided modes are equally excited and disregarding chromatic dispersion, the transit time difference between the fastest and slowest mode is

$$\delta\tau_{max} = \begin{cases} \frac{n_o L}{c} \cdot \Delta(\alpha - \alpha_o)/(\alpha+2), & \text{for } \alpha \neq \alpha_o \\ \frac{n_o L}{c}\frac{\Delta^2}{2}, & \text{for } \alpha = \alpha_o \end{cases} \qquad (45)$$

where $\alpha_o = 2 - \frac{2.\lambda}{\Delta}\frac{d\Delta}{d\lambda}$

The above result shows an optimization in propagation times when the index profile has a nearly parabolic shape. The improvement from a step index fiber ($\alpha \sim \infty$) to a graded fiber with $\alpha = \alpha_o$ is of the order of $2/\Delta$ or 200 times.

If an optical signal with a pulse shape given P(t) is injected in a fiber, the output shape $P_o(t)$ is given by

$$P_o(t) = \int_{-\infty}^{+\infty} P_i(t')h(t-t')\,dt' \qquad (46)$$

where h(t) is the impulse response of the fiber and where all the broadening effects discussed so far, are contained. The objective of the measurement is then to obtain this important function. Assuming that the fiber is a linear system we can define a set of Fourier transforms $P_o(w)$, $H(w)$ and $P_i(w)$ from the correspondent $P_o(t)$, $h(t)$ and $P_i(t)$. The relation between them is

$$P_o(w) = H(w) \cdot P_i(w) \cdot \qquad (47)$$

H(w) is the frequency response of the fiber and gives the attenuation of every baseband frequency w, since the fiber, as a passive device, can be regarded as a low pass filter.

Some useful relations can be further defined, if the input pulse $P_i(t)$ and fiber response h(t) are the following Gaussian functions

$$P_i(t) = \exp\left(-4.\ln 2.(t/\sigma_i)^2\right) \qquad (48)$$

$$h(t) = \exp\left(-4.\ln 2.(t/\sigma_F)^2\right) \qquad (49)$$

Then, by Eq. (46) P is also a Gaussian with a width at half maximum σ_o. The fiber response width is then

$$\sigma_F^2 = \sigma_o^2 - \sigma_i^2 \qquad (50)$$

Using Fourier integrals, it can be shown that $P_o(w)$, $H(w)$ and $P_i(w)$ are also Gaussian functions. The point in which the frequency response attenuation is - 3 dB (half intensity), that is defined as the fiber bandwidth B_w is

$$B_w = \frac{0.44}{\sigma_F} . \qquad (51)$$

This relation permits a rapid calculation of the fiber bandwidth from the pulse broadening if its shape is nearly Gaussian.

Finally, if there is an extra broadening effect given by the chromatic dispersion and if the source spectral line shape is also Gaussian, the total fiber response half width (σ_T) is

$$\sigma_T^2 = \sigma_F^2 + \sigma_c^2 \qquad (52)$$

where σ_c is the pulse width given by chromatic effects.

In the following sections, the most used methods for measuring multimode fiber bandwidth and chromatic pulse dispersion will be described.

5.2. TIME DOMAIN TECHNIQUE

The basic idea here is to inject, in the fiber, an optical pulse with a known shape and measure the output pulse on the other end. Fiber response is then computed simple by using Eq. (50) or else by doing a more elaborate analysis on the pulse shapes, such as RMS (root mean square) widths which will obey a equation similar to Eq. (50). Another procedure, more common, is to calcualte the frequency response curve H(w) from Eq. (47) once the Fourier transform of the input and output pulses are known.

The experimental system to conduct these measurements is shown in Figure 25. A pulsed laser diode of the desired wavelength is used to generate the subnanosecond optical pulse, that is sent into the fiber test through a launching fiber, for a controlled mode excitation. The output light is focused into a fast response detector with the help of an infrared viewer and a couple of microscope objectives. Due to the very narrow pulse widths involved, less than 1 nanosecond for good fibers, the pulse shape is measured with a time scanning sampling

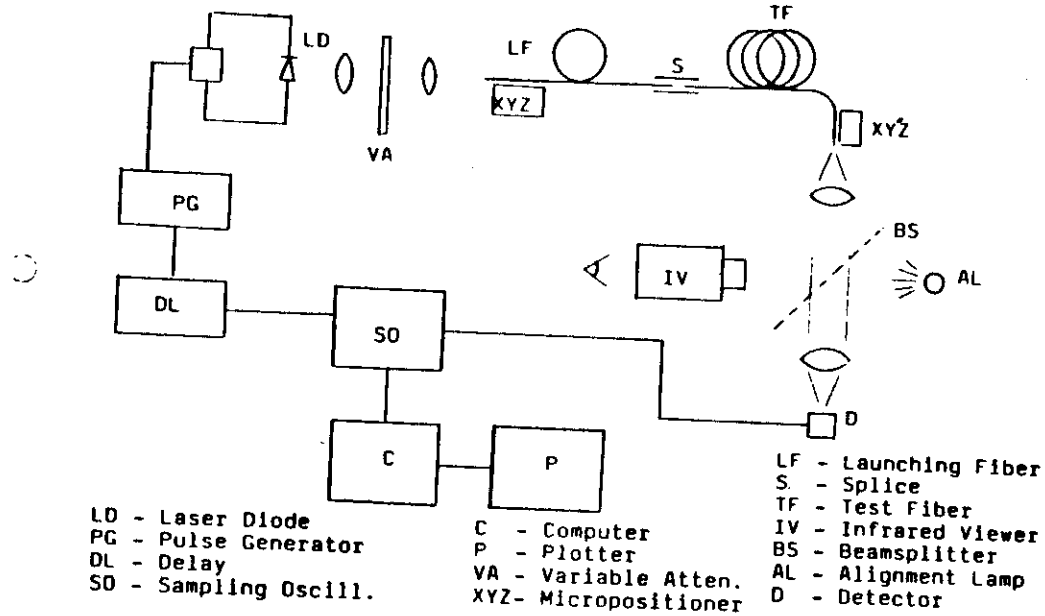

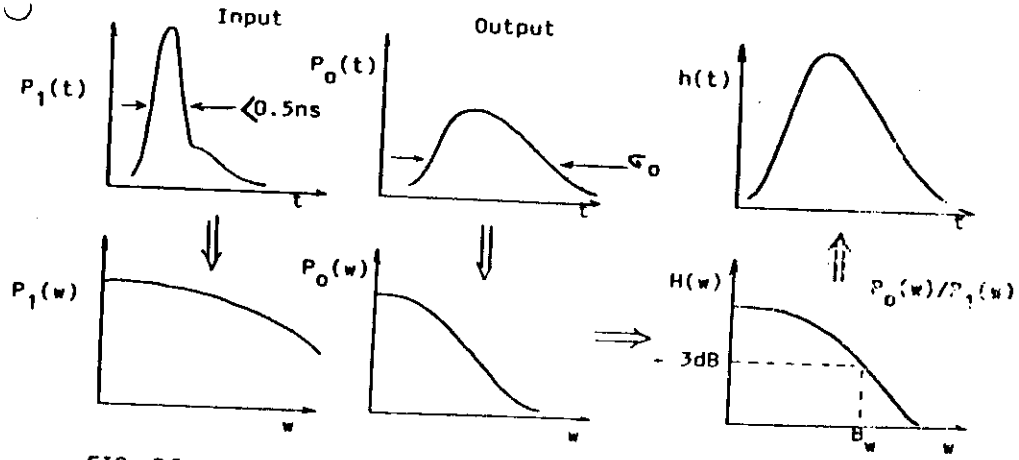

FIG. 25 - Experimental set-up and waveform processing for fiber bandwidth ----

oscilloscope. Because of the pulse propagation delay through the fiber, the input pulse trigger must be delayed before the oscilloscope. Pulse shapes are then stored in a digital memory for posterior analysis. It is important to use an opical attenuator for the measurement of the input pulse, so the same electronics gain is always used to preserve system linearity. The Fourier transformation indicated in Figure 25, is usually done with Fast Fourier Transform Techniques, once the two pulse shapes are stored.

An example of a measured pulse is shown in Figure 26. The input pulse had a 200 ps width at half maximum. The calculated fiber frequency response curve, calculated with a FFT routine is also shown. In this graph, the 0 dB normalization was done at 10 MHz.

In the 1.3 ~ 1.5 μm region, the chromatic dispersion for multimode fiber is small in comparison with modal dispersion. For measurements in the 0.85 μm region, the chromatic effect can be taken out from the frequency response curve and Gaussian approximations, are usually employed in this deconvolution process.

In terms of light sources and detectors, in the 0.85 μm region, GaAs laser diodes and fast silicon APD (avalanche photodetector) detectors are employed. Around 1.3 - 1.55 um, InGaAsP lasers and germanium APD or PIN InGaAs detectors are the best. Typical laser pulse width is around 200-400ps with a 3 nm spectral line. The detectors bandwidth should exceed a few GHz.

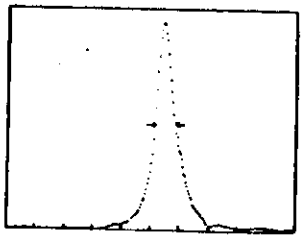

(a)

Time (1 ns/div)

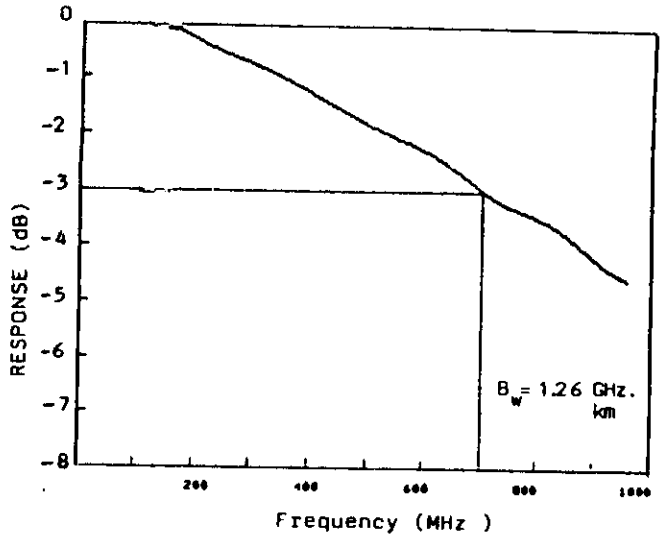

(b)

FIG. 26 - Bandwidth measurement in the time domain. (a) output pulse at λ = 1.3 microns and 17km fiber length; (b) frequency response curve by FFT processing.

Various other triggering techniques, apart from the one shown in Figure 25, can also be used. A specially interesting case, is when the two fiber ends are not available in the same place. An auto triggering scheme can be used if there is enough signal for that. Another way for not having triggering problems and to obtain immediately the frequency spectrum of pulses, is to use an spectrum analyzer in place of the sampling oscilloscope.

Concerning launch conditions the same care as used for attenuation measurements must be taken. But due to mode coupling and other effects, the situation is more critical in this case. In the set-up shown in Figure 25, a length of step index fiber with a core diameter and numerical aperture slightly inferior to the test fiber is used for launching the light.

5.3. FREQUENCY DOMAIN MEASUREMENT

In this technique, a sinusoidally modulated light is launched into the fiber and the modulation amplitude of the output signal is measured and compared with the input. To determine the fiber response over a certain frequency range, the measurement is made for a set of frequencies within the limits. The frequency response of the measuring system by itself must be extracted out of the data. To do so, a measurement with a short piece of fiber is done and the fiber response calculated using Eq. (47).

The basic experimental arrangement to conduct frequency domain measurements is shown in Figure 27. The launch and detection optics is the same as in the other technique (Figure

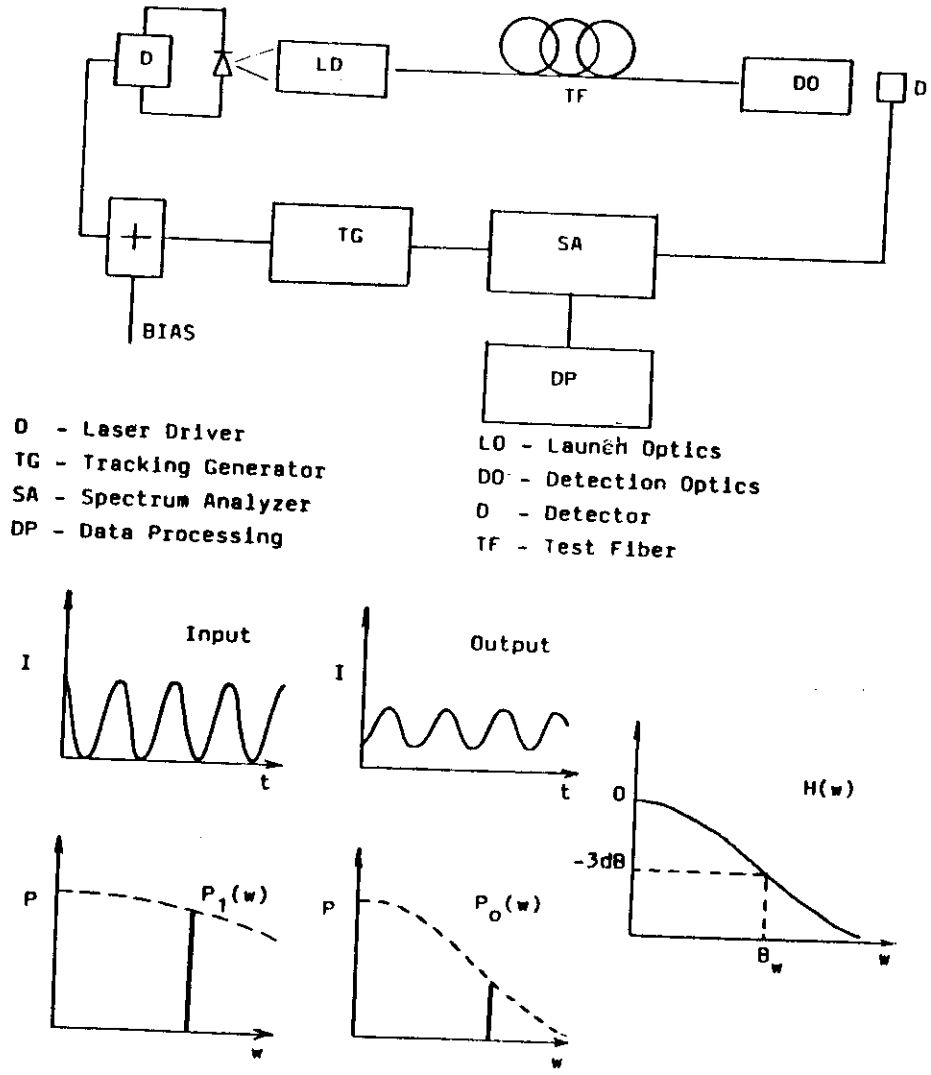

FIG. 27 - Experimental set-up and method for measuring fiber bandwidth in the frequency domain.

25). The laser used must be one capable of operating in a continuous modulati· , from about 10 MHz to 1 GHz. The data taking and processing method is also shown in the figure. The frequencies are sweeped in the given range by a tracking generator connected to a spectrum analyzer. A variation of this method, that don't need any input-output side synchronization, consist of doing the data taking, frequency by frequency just using a tunable wideband signal generator. This can be done manually or in some automatic scheme. For field use then the two fiber ends are not in the same loca tion, any of these methods needs to be used.

A comparison between time and frequency domain measurements techniques, show that both are equivalent in terms of results, with precision around 5 to 10%. Time domain has a better frequency range but requires a Fourier transform operation. Frequency domain has a better dynamic range and is a direct method, as far as fiber frequency response curve is concern.

A final point about multimode fiber bandwidth that needs to be mentioned, is its wavelength dependence. From Eq. (45) it's clear that the optimum fiber index profile parameter (α) depends on wavelength, because of profile dispersion ($\frac{\lambda}{\Delta}\frac{d\Delta}{d\lambda} \simeq f(\lambda)$). If laser diodes or any other light source with different emission wavelengths are used in any of the above described methods, a graph of bandwidth versus wavelength can be made. In Figure 28 we have an example of this curve for three different fibers each with its own fitting deviation (χ) from an ideal α , Δ profile. We see immediately that the lowest χ value fiber, has a clearly

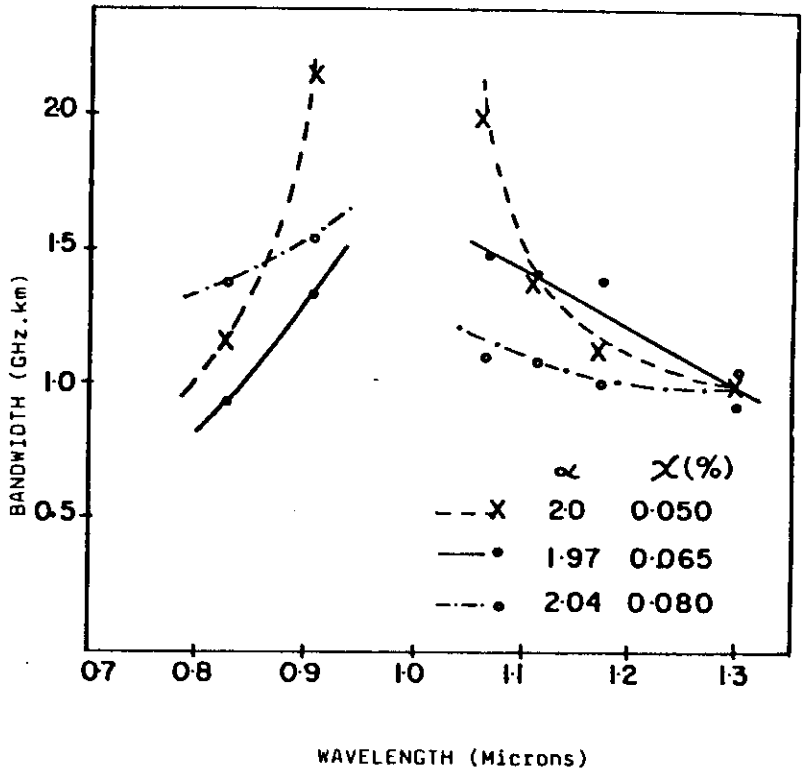

FIG. 28 - Fiber bandwidth as a function of wavelength for three different fibers with the index profile parameters given above.

defined optimization wavelength, this being not so true for the others even though they are very high performance fibers that can be used in both windows, .85 μm and 1.3 μm. In the results shown in Fig. 28, chromatic dispersion effects were taken out. When this contribution is added up, for typical spectral line widths of common lasers around 5nm, the total bandwidth at the 0.85 μm region will be reduced. Near 1.3 μm this effect is negligible.

5.4. CHROMATIC DISPERSION MEASUREMENTS

As it was already discussed, chromatic dispersion of light pulses propagating in an optical fiber occurs because the group velocity depends on wavelength. For multimode fiber, this effect adds to the modal dispersion and for monomode fibers, it is the only limitation to the transmission bandwidth . So, the most obvious way of measuring this effect, on any kind of fiber, is to detect the difference on propagation times (τ) of light pulses with different wavelengths. Chromatic dispersion is then defined as

$$M(\lambda) = \frac{\frac{d\tau}{d\lambda}}{L} \qquad (53)$$

and is normally given in ps/nm.km.

In Figure 29 the basic experimental set-up for this measurement is shown. A variable wavelength pulsed light source, sends two or more light pulses into the fiber through some kind

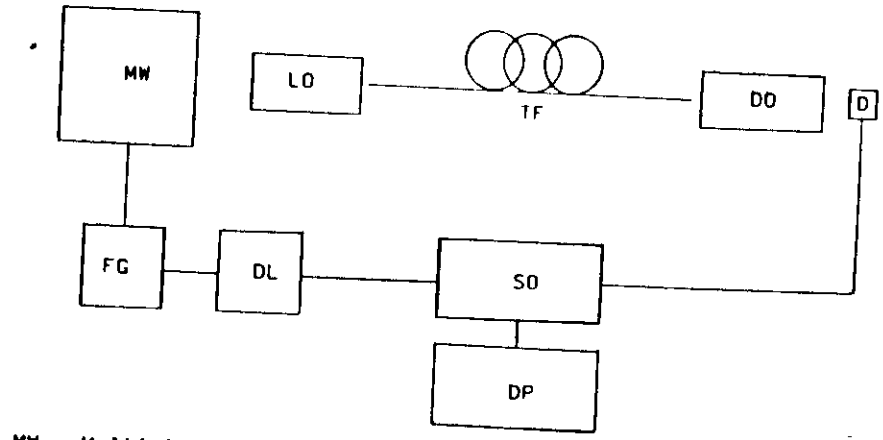

MW - Multiple Wavelength Pulsed Light Source
FG - Frequency Generator
DL - Delay
SO - Sampling Oscilloscope
DP - Data Processing
LO - Launch Optics
DO - Detection Optics
D - Detector
TF - Test Fiber

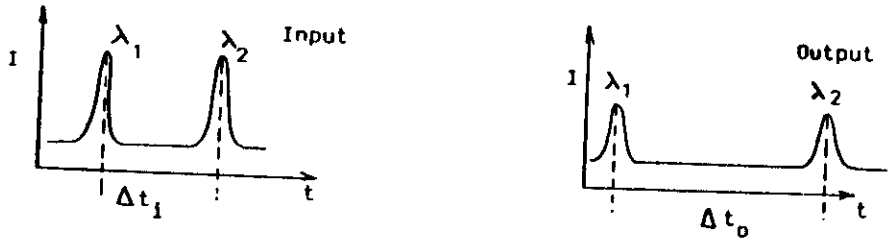

$$M = \frac{(\Delta t_i - \Delta t_o)}{L\ (\lambda_1 - \lambda_2)}$$

FIG. 29 - Measurement of chromatic dispersion by the propagation delay method.

of launching optics (not critical in this measurement). The detection optics and detectors are of the same kind of the ones described in sections 5.2 and 5.3. The time difference between the pulses, before and after propagating in the fiber, are measured and chromatic dispersion calculated from Eq. (53).

The light source used in this type of measurements can be of various kinds. The most used configurations are given in Figure 30. The simplest one is to used two laser diodes and a beamsplitter to combine their outputs. Each one emits a short pulse (< 1ns) triggered by a low frequency pulse generator. Another configuration uses various lasers, which outputs are combined into the fiber using a fiber coupler, thus making a very compact system.

A very versatile variable wavelength pulse light source is by means of a high power Nd:YAG laser, pumping short pulses into a monomode silica fiber and generating a Raman spectrum as shown in Figure 30.

The desired wavelength is selected by means of a monochromator and this set-up offers a large selection of wavelengths, over the most interesting region for monomode fibers, from 1 to 1.5 microns. Anti-Stokes Raman lines, for wavelengths smaller than the Nd:YAG emission, at 1.06 um, is also available, but with less intensity, all the way down to 0.5 microns. In this apparatus, the signal used for triggering purposes is normally obtained from the rear end beam of the laser with a convenient delay line.

A result, using the Raman laser, is given in Figure 31. The

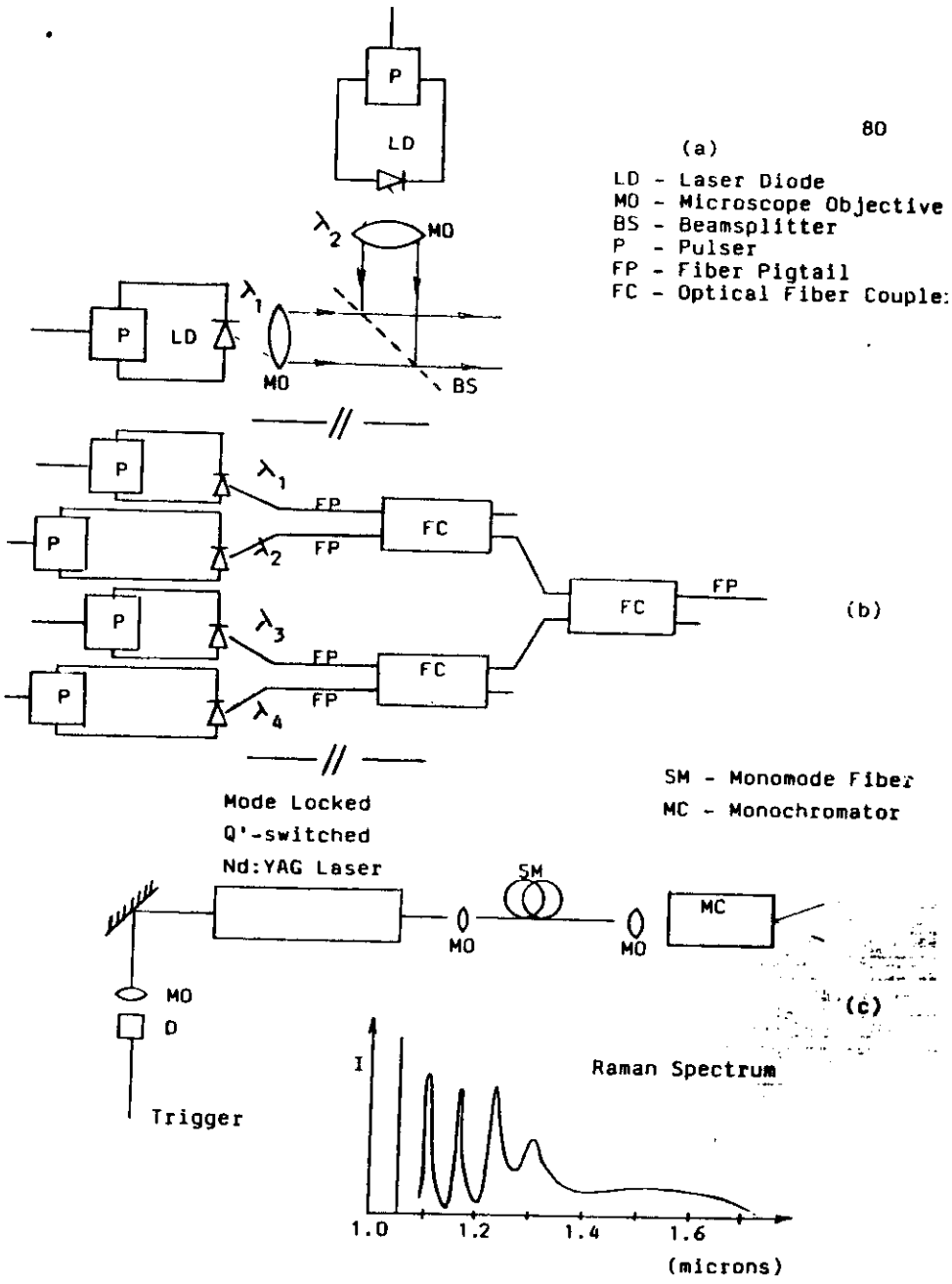

FIG. 30 - Multiple wavelength pulsed light sources for chromatic dispersion measurement in time domain.

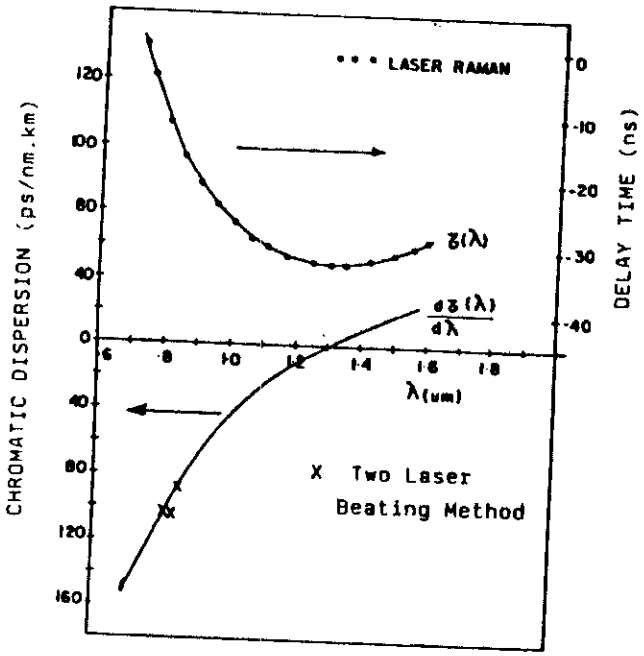

FIG. 31 - Chromatic delay and dispersion measurement of a multimode graded index fiber using a Raman laser source.

time delays at the various wavelengths, were plotted with respect to the 0.72 microns pulse. The derivative of this curve i.e the chromatic dispersion is also shown. The λ_o wavelength, corresponding to the point where $M(\lambda)$ is zero, is very important in monomode fiber design. Depending on the waveguide dispersion effect, in Eq. (44), this λ_o can be moved around, from 1.2 to even 1.55 microns, thus opening the possibility of making monomode fibers with almost infinite bandwidths at any wavelength.

The Raman laser configuration just described offers large intensity pulses at almost any wavelengthof interest. On the other hand, this system is very bulky, dangerous, expensive and suffers from jitter and different instabilities. It is most appropriate for laboratory environment. The other configurations are also limited in terms of availability of diode laser lines to cover a wide range but the system can be made very compact and simple to use.

Some other measurements techniques based on detecting modulated signals instead of pulses, are being also used. If a sinusoidal modulated signal propagates down the fiber, the detected intensity will be

$$P = P_o \cos (\omega t + \phi_o) \qquad (54)$$

where ω is the frequency and ϕ_o any constant phase. When the wavelength changes by $\Delta\lambda$, for a given frequency, the change in

phase is

$$\Delta\phi = w \frac{dt}{d\lambda} \Delta\lambda + \frac{\partial \phi_o}{\partial \lambda} \Delta\lambda \qquad (55)$$

From (53) we have then

$$M(\lambda) = \frac{1}{wL}\left[\frac{d\phi}{d\lambda} - \frac{\partial_o}{\partial\lambda}\right] \qquad (56)$$

Thus, the chromatic dispersion can be determined by measuring the phase shift as a function of wavelength. The second term in Eq. (56) is a systematic experimental parameter that can be determined in a separate experiment in which only a small length of fiber is measured.

To perform this phase shift measurements, the same type of apparatus as shown in Figure 29 can be used, substituting the oscilloscope by a phase sensitive detector such as an vector voltmeter and disregarding the delay line. Usually modulation frequencies above a few tens of MHz are needed to have an apreciably phase change, since the phase shift is proportional to w. The light source employed can be one or more LED's to cover the region of interest with a monochromator for wavelength selection, or various laser diodes with different wavelength (see Figure 30b).

Also, with respect to frequency domain techniques, if two

lasers with different wavelengths are modulated synchronously, the detected signal plotted as a function of frequency will be modulated by cos ($w\Delta t$) where Δt is the difference in delay time between the two wavelengths as shown in Figure 32. A experimental value obtained with this technique is shown in Figure 31, and it compares well with the Raman laser technique.

Finally, it must be emphasized here, that all the above described methods apply for multimode and for monomode fibers, where chromatic dispersion is the critical parameter limiting fiber bandwidth.

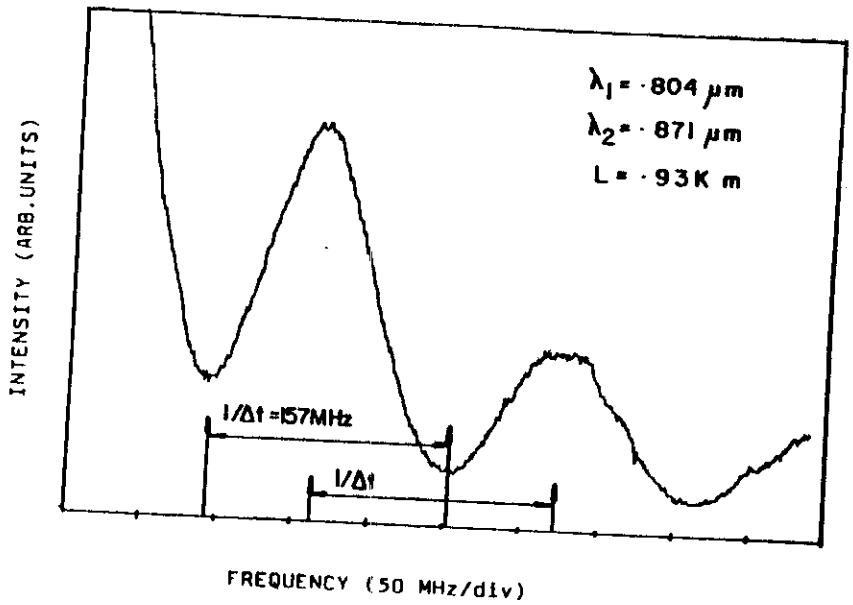

FIG. 32 - Beating of two frequency modulated laser signal with different wavelengths, after propagating in an optical fiber.

6. MEASUREMENT OF MONOMODE FIBER PARAMETERS

6.1. INTRODUCTION

All measuring techniques described so far are applicable to multimode as well for monomode fibers. For this last type of light guide, there are two more measurements that needs to be made. One of them is the determination of the wavelength above which, only the fundamental mode, the LP_{01}, is present. The other one, is the characterization of the field distribution of the fundamental mode, particularly its diameter. The knowledge of this value, at a given wavelength, permits one to evaluate the splicing characteristics of the fiber and its sensitivity to microbending loss, induced by cabling and lay out. If the dependence of the mode diameter with wavelength is known, the cut-off wavelength as well as the waveguide dispersion can be also obtained.

But before we go through the details of the specific measuring techniques, some of the basic relationship for the parameters of the fundamental mode will be given.

6.2. FUNDAMENTAL MODE BASIC RELATIONS

The index of refraction profile of a monomode fiber can be of any shape, either non-intentionally because of fabrication limitations or to optimize some fiber characteristics such as loss or dispersion properties. But generally, the fundamental mode shape will not depend very strongly on the exact index profile, since the spatial dimensions involved are of the order of the wavelength itself.

The field distribution for the step index profile can be exactly calculated as well as other parameters such as cut off wavelength and dispersion. If the core index is given by Δn and its radius by a, the cut off wavelength is then

$$\lambda_c = \frac{2\pi a \sqrt{2n_o \Delta n}}{2.405} \qquad (57)$$

This is the theoretical value that holds only for ideal conditions. In reality, since the field distribution of the second order mode (LP_{11}) extends out in the cladding, the loss of this mode is very sensitive to micro and macrobending, specially near the cut-off region. So in practice, there exist an effective cut-off wavelength that depends on fiber length, index profile, curvature and other extrinsic conditions.

Even though , the fundamental mode field distribution is not exactly Gaussian, this analytical representation gives a very good approximation, specially inside the core. Thus, the transverse field can be represented by

$$E(r) = Eo \cdot \exp\left(-\frac{r^2}{w_o^2}\right) \qquad (58)$$

where w_o is the spot radius at $1/e^2$ of the intensity distribution.

When Eq (58) is confronted with the exact field distribution, the dependence of w_o with other fiber parameters can be determined

$$w_o = a\left[0.65 + 0.434\left(\frac{\lambda}{\lambda_c}\right)^{3/2} + 0.149\left(\frac{\lambda}{\lambda_c}\right)^{6}\right] \qquad (59)$$

This expression, known as the Marcuse relation, permits the determination of fiber parameters a and λ_c once the wavelength dependence of w_o is known.

When the index profile of a given fiber, is not a step function, the fundamental mode field distribution still resembles a Gaussian function and so the fiber characteristic can be approximate by an equivalent step index fiber. Of course, this type of approximation is not to be used for very accurate purposes but only for a first glance. Anyhow, for graded index profile with and without the central dip, this approach works very well.

In the equivalent step index approximation, the equivalent radius and index difference are given by

$$a_e = 2\frac{\int_o^\infty \Delta n(r) r\,dr}{\int_o^\infty n(r)\,dr} \qquad (60)$$

and

$$n_e = \frac{\int_0^{\infty} \Delta n(r)\,dr}{a_e} \qquad (61)$$

where $\Delta n(r)$ is the measured index of refraction difference between core and cladding. Thus, if these effective parameters are used, all the other relationship may be employed, by substituting a and Δn by the above values.

6.3. CUT-OFF WAVELENGTH MEASUREMENT

There are two basic methods of measuring cut off wavelength. One of them consist of determining the wavelength in which the loss of the second mode increases abruptly. This can be detected by comparing fiber transmission with and without a bend around a mandrel. Comparing the transmission curves between a multimode and the single mode test fiber, will also detected this increase in loss. The other method is by measuring the diameter of the mode field as a function of wavelength. In this technique, by decreasing the wavelength,where the mode field is measured, there will be a point in which the field of the second mode will superimpose the fundamental one that is very much confined in the core at this point. The measured field will increase abruptly just at the cut-off point and eventually stabilize at a given value and then slowly decrease again as it gets more concentrated in the core.

In this section, we will describe just the first method and comment the other one at the next section.

To measure the cut-off wavelength by detecting the high loss point of the LP_{11} mode, an experimental set up similar to the one employed for attenuation measurements is used. An schematic of the measuring system is given in Figure 33. To avoid exerting any constraint, such as clamping down the test fiber, that will induced any non controlled increase of the LP_{11} loss, it is better to splice it to multimode fibers in the input and output ends. The first recording of transmission intensity versus wavelength is conducted with the whole length of the fiber (1-2m) completely straight and without any external pressure on it. For the second measurement, a single loop of radius R (16cm or any other value) is made. In drawing (a) both measurements are shown and the log of the ratio is plotted. The cut-off wavelength is the far right point shown. If the value of R is changed, the far left point of the curve will change as shown.

If the reference transmission is not done, with the bent fiber, but with a multimode fiber (can be the same as the spliced fiber MF) the results will be as given by (b) in Figure 33. a real measurement curve is shown in Figure 34. Apart from the λ_c point in $\lambda = 1.28\ \mu m$, the cut off wavelength of the third mode is evident at $\lambda = 0.84$. This is confirmed by the fact that the two cut-off wavelengths ratio (0.84/1.28 = 0.66) is the same as ratio of theoretical cut-off V values for the LP_{11} and LP_{21} + LP_{02} modes, i.e 2.405 and 3.832 (2.405/3.832 = 0.63).

Another interesting feature is the 4.8 dB transition near

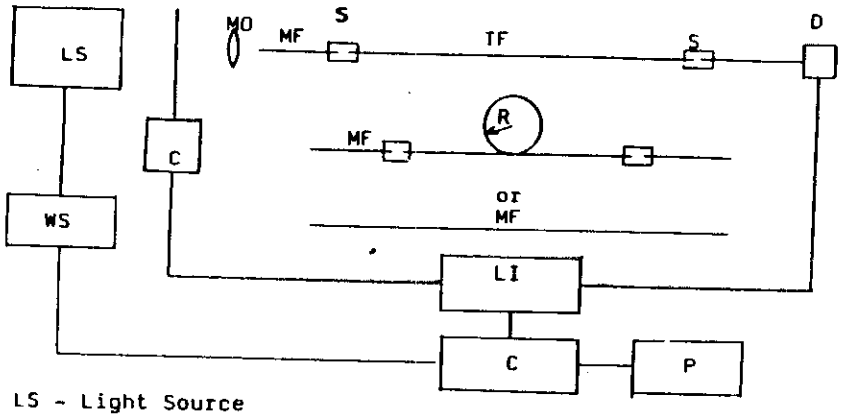

LS - Light Source
WS - Wavelength Selector
CH - Chopper
LI - Lock-in Amplifier
C - Computer
P - Plotter

MO - Microscope Objective
S - Splice
D - Detector
TF - Test Fiber
MF - Multimode Fiber

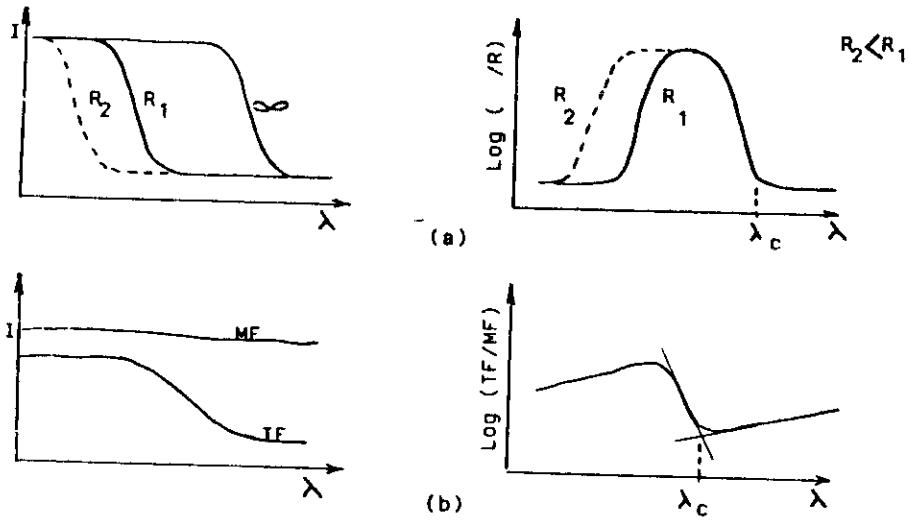

FIG. 33 - Experimental set-up for measuring cut-off wavelength. (a) bending method; (b) multimode fiber comparison.

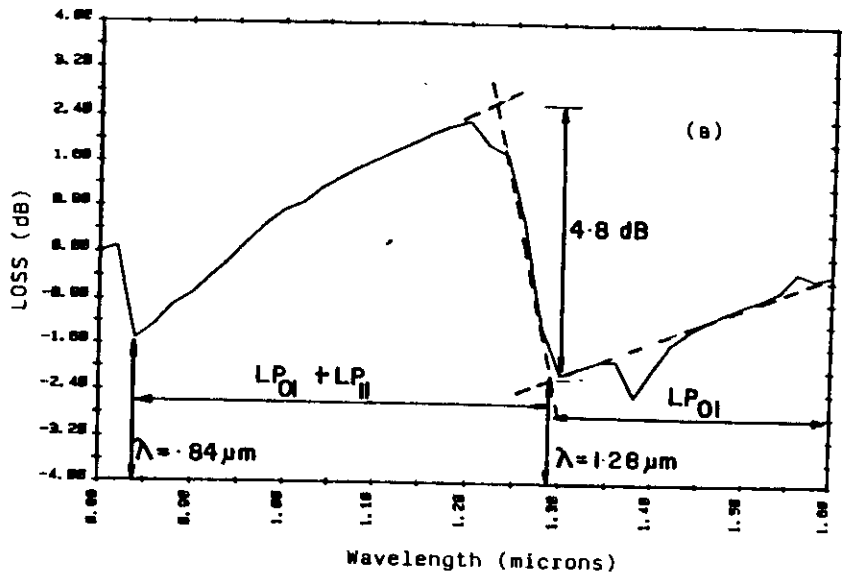

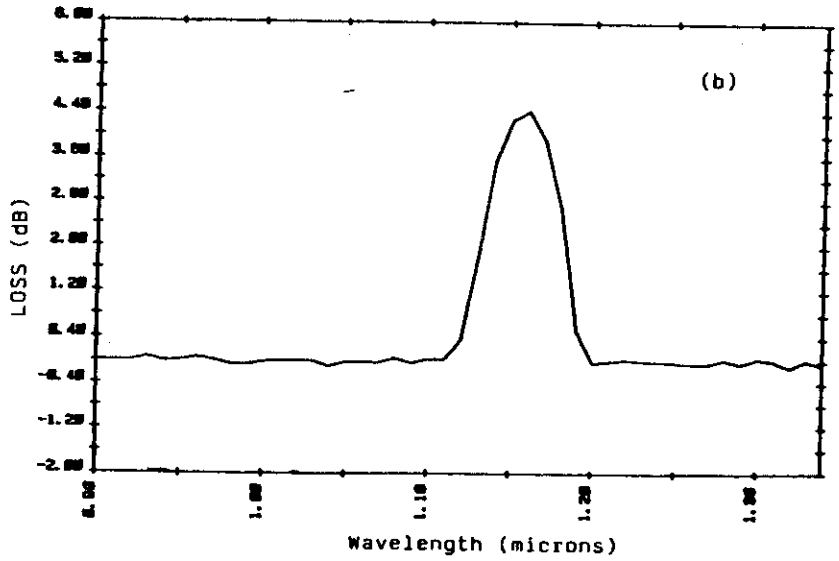

FIG. 34 - Cut-off wavelength measurements by the transmission method: (a) compared with a multimode fiber and (b) with a bend of R ~ 16cm (not the same fiber in the two plots).

λ_c. Since the mode degeneracy of the LP_{01} and LP_{11} modes is 2 and 4 respectively, the ratio of power carrying modes is 2+4/2 = 3 or 4.77 dB. If equal mode excitation is assumed, then it follows what is seen in Figure 34.

As would be expected, the cut off wavelength is a function of fiber length and curvature. This dependence is shown in Figure 35 and can be parametrized for step index profiles) as

$$\lambda_{c\,eff} = \lambda_c\,(L = 1,\ R = \infty) - A \log (L) - B/R \qquad (62)$$

where L is the fiber length, R the curvature radius and the A and B constants, that depend on fiber type, cabling and other conditions. This shows that it is very important in any λ_c determination to specify completely the conditions in which the measurements were performed.

6.4. MODE FIELD DIAMETER MEASUREMENT

The most obvious way of measuring the mode field distribution and its diameter is by performing a near field scanning in the same way as described in section 3.2. Assuming a Gaussian field as given by Eq. (58) the nearfield data is fitted to this expression to yield w_o. The fitting criteria is one that would maximize the coupling between a Gaussian and the real field distribution. So, the integral to be maximized is the following:

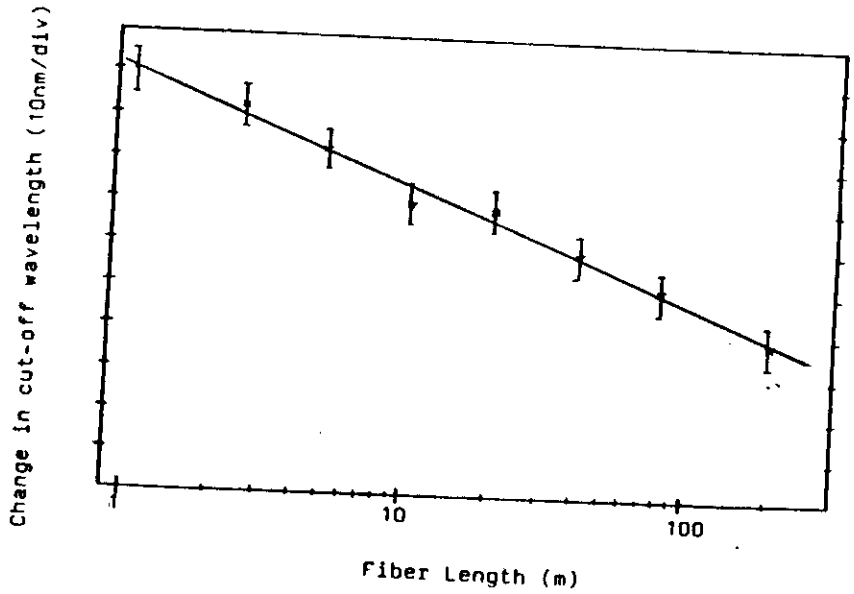

FIG. 35 - Change in the measured cut-off wavelength as a function of fiber length.

$$I = \frac{\left[\int_0^{\infty} rf(r)\ E(r)dr\right]^2}{\int_0^{\infty} rf(r^2)\ dr \cdot \int_0^{\infty} eE(r)dr} \qquad (63)$$

where f(r) is the square root of the measured near field data.

Apart from being a very direct method, the near field scanning is not an easy measurement to be done, specially if the wavelength dependence of w_o is sought. Among the problems are, focusing for every λ and low detected power (poor signal to noise ratio)

A variation of the near field is to do the more easy one, far field scan. There are mathematical ways of transforming far field distribution to the correspondent near field and the same procedures as given above are executed. But this is a rather messy calculations and a more direct way is to fit a Gaussian transformed field distribution to the actual far field data. The fitting criterium in now to maximize,

$$I = \frac{\left[\int_0^{\infty} \Theta\, E(\Theta).\ g(\Theta)\ d\Theta\right]^2}{\int_0^{\infty} E(\Theta)\ d\Theta \cdot \int_0^{\infty} g(\Theta)\ d\Theta} \qquad (64)$$

where Θ is the far field angle and $g(\Theta)$ is the square root angular power distribution and

$$E(\Theta) = Eo\ e^{-\Theta^2/\Theta_w^2} \qquad (65)$$

Once the Θ_w value is obtained from the fitting, the mode radius is given by

$$w_o = \frac{\lambda}{\pi.\tan\Theta_w} \qquad (66)$$

The experimental set-up to perform far field scan in monomode fiber is the same as the one shown in Figure 7. This technique also suffers from low detected signal as in the case of all monomode fiber measurements.

A very direct way, as far as fiber splicing is concern, to measure mode field diameter, is the transverse offset method. In this case, the fiber is cut in two pieces, couple face to face and the transmission through this interface is measured as a function of transverse offset. Assuming Gaussian fields, the transmission as a function of offset d is then

$$T(d) = To.e^{-\left[\frac{d}{w_o}\right]^2} \qquad (67)$$

Thus, doing a simple fitting of Eq. (67) to the measured data will give the mode field diameter $2w_o$.

The implementation of this measurement is done using the same apparatus as for in attenuation measurement with the addition of two travelling stages as shown in Figure 36. The same splicing to a multimode fiber for light launching purposes is also done as in the λ_c measurement. A typical transverse scan for a given wavelength is shown in Figure 37(a). One can see that the Gaussian function (67) fits very well to the measured data. The variation of the mode diameter with wavelength is in Figure 37(b). The cut-off wavelength is very clearly shown.

The increase in $2w_o$ with wavelength, as given by Eq. (59) is also apparent. Fitting these data with this equation is an alternative way of obtaining fiber parameter such as λ_c and equivalent radius a_e, from Eq. 57, Δn_e is then calculated.

There are other methods for determining the mode diameter that don't rely on the Gaussian approximation, in which all the above techniques are based. This is particularly important issue for fibers that have exotic profiles needed for dispersion curve shifting and flattening. But since they are not yet stablished techniques we will not go into more details.

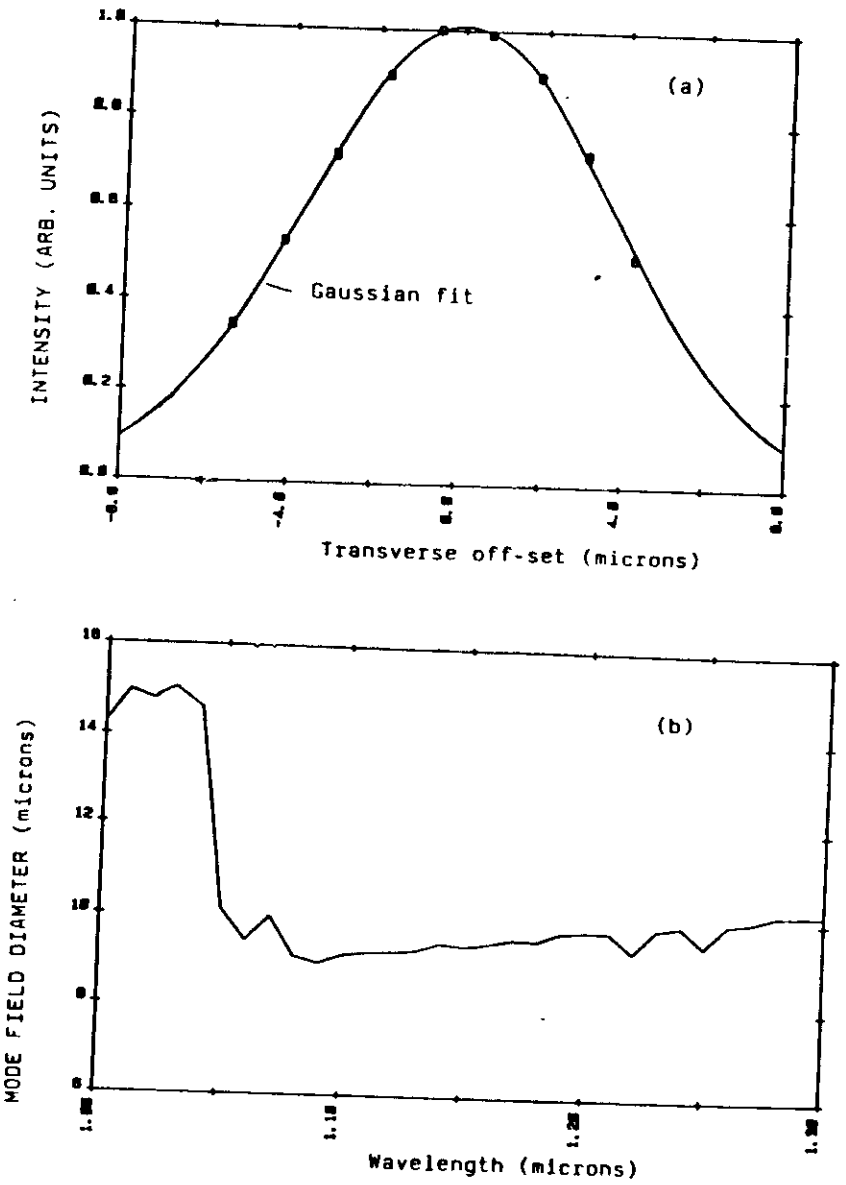

FIG. 37 - Mode field diameter measurement by the transverse off-set method. (a) transmission power as a function of off-set; (b) mode diameter as a function of wavelength.

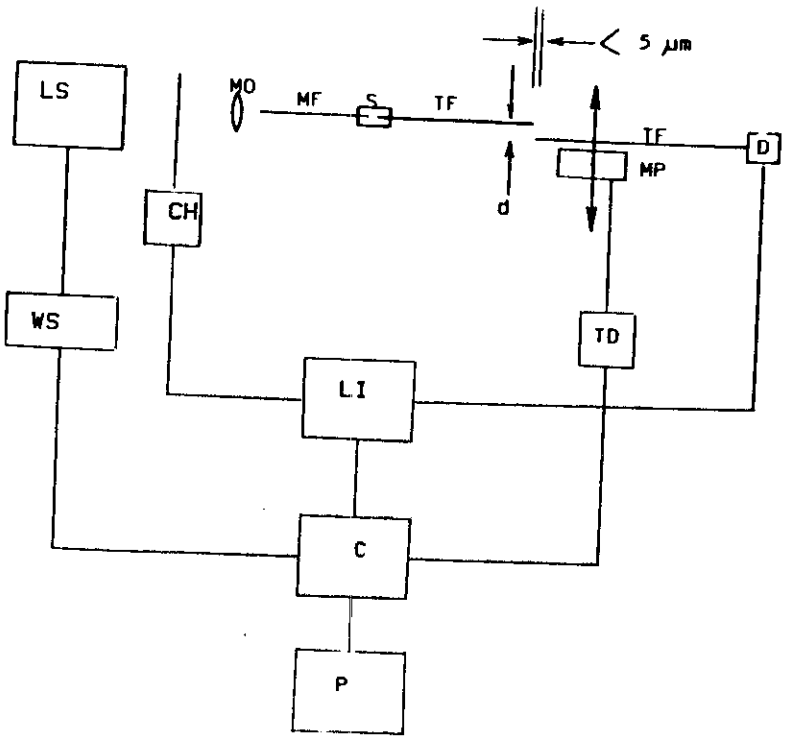

LS - Light Source
CH - Chopper
WS - Wavelength Selection
LI - Lock-in Amplifier
C - Computer
P - Plotter

MO - Microscope Objective
S - Splice
D - Detector
TD - Translation Driver
MP - Motorized Micropositioner
MF - Multimode Fiber
TF - Test Fiber

FIG. 36 - Experimental set-up for measuring mode field diameter by the transverse offset method.

7. CONCLUSIONS

Throughout this text we tried to cover most of the optical measuring techniques that are used today in fiber optics technology. Many other techniques, even though very interesting ones, were not mentioned here rather because they are outdated or still in its infancy and subjected to many studies. Now, the main objective of people involved in this field is to find ways of getting reliable results in the most simplest way. This is very important, since fiber optics are getting out the laboratories and into the commercial world. In this setting cost and performance will eventually determine the full applicability of optical commmunications technology in the future.

8. REFERENCES AND BIBLIOGRAPHY

1. Optical Fiber Telecommunications, S.E.Miller and A.G.Chynoweth Eds, 1979, Academic Press, New York, USA.

2. Principles of Optical Fiber Measurement, D. Marcuse, 1981, Academic Press, New York, USA.

3. Optical Fiber Characterization, National Bureau of Standards Special Publication 637, volumes 1 and 2, 1982, U.S Government Printing Office, Washington D.C, USA.

4. Optical Fibre Communication, Technical Staff of CSELT, 1980, CSELT, Turin, Italy.

5. CCITT Recommendations G651 and G652, Study Group XV.

6. Measurements in Fiber Optics, M.Barnoski and S.D.Personick, Proceedings of the I.E.E.E., vol. 66, n° 4, p.429, 1978.

7. Single Mode Fiber Optics, L.B.Jeunhomme, 1983, Marcel Dekker Inc., New York, USA.

8. Technical Digest of the Symposium on Optical Fiber Measurements, 1980, 1982 and 1984, National Bureau of Standards Special Publications 597, 641 and 683. U.S. Government Printing Office, Washington D.C., USA.